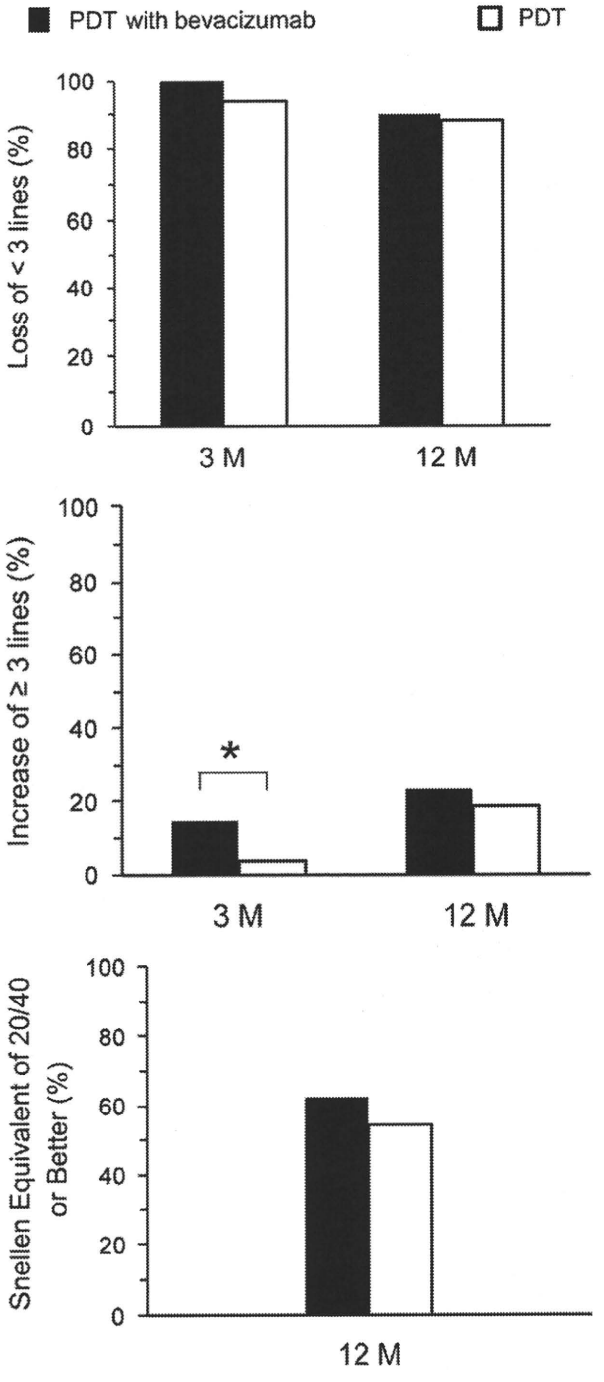

FIGURE 2. Bar graphs showing the rates of eyes with losses or gains in visual acuity at 3 and 12 months (M) and with a best-corrected visual acuity (BCVA) with a Snellen equivalent of 20/40 or better at 12 months associated with photodynamic therapy (PDT) combined with intravitreal bevacizumab compared with PDT monotherapy for polypoidal choroidal vasculopathy. (Top) Percentage of eyes in each group with improved or maintained BCVA (a loss of fewer than 3 lines of vision). The rates do not differ significantly between the groups. (Middle) Percentage of eyes with improved BCVA of 3 lines or more. The rate in the PDT combined with bevacizumab group is significantly ($P = .044$) higher than in the PDT group at 3 months. However, the rates do not differ significantly at 12 months. (Bottom) Percentages of eyes with a BCVA of 20/40 or better at 12 months. The rates do not differ significantly.

Eyes gained a mean of 0.12 logMAR unit (1.2 lines) in the combined therapy group and 0.04 logMAR unit (0.4 lines) in the PDT monotherapy group over 12 months. All eyes (100%) in the combined therapy group and 80 eyes (94.1%) in the PDT monotherapy group had improved or stable VA (defined as a loss of 3 or fewer lines of vision at 3 months); the rates were 90.2% (55/61) and 88.2% (75/85) at 12 months, respectively, in the treatment groups. An improvement in the BCVA of 3 lines or more was seen in 14.8% (8/44) in the combined therapy group and in 3.5% (4/79) in the PDT monotherapy group at 3 months, which was significant (Fisher exact test, $P = .044$); however, the respective rates were 23.0% and 18.8% at 12 months, which were not significant. The percentages of eyes with a BCVA of 20/40 or better at 12 months was 62.3% in the combined therapy group and 54.1% in the monotherapy group (Figure 2).

To elucidate factors associated with the long-term BCVA, we performed multivariate analyses. Based on stepwise regression analyses, the baseline BCVA ($P < .0001$), the GLD ($P = .0015$), PED ($P = .0022$), and treatment ($P = .048$) significantly affected the BCVA at 12 months. Therefore, the better BCVA at 12 months was correlated with a higher baseline BCVA, smaller GLD, no baseline PED, and the combined treatment. The combined therapy also was identified as a factor associated with a BCVA at 12 months of 20/40 or better from the logistic regression analysis (odds ratio, 2.66; $P = .040$), in addition to better baseline BCVA ($P < .0001$), no baseline PED ($P = .0072$), and smaller GLD ($P = .0094$).

• CHANGES IN LESIONS AND ADDITIONAL TREATMENTS: After the initial treatment, the resolution of lesions at 3 months was confirmed in 78.7% (48/61) of eyes in the combined therapy group and in 75.3% (64/85) of eyes in the monotherapy group. Among those eyes, the lesions recurred in 43.8% (21/48) of eyes in the combined therapy group and 40.6% (26/64) in the PDT monotherapy group during the 1-year follow-up. These rates did not differ significantly between treatments ($P = .63$, $P = .74$, Pearson chi-square test). During the 1-year follow-up, a mean of 0.43 PDT and 0.92 bevacizumab additional injections in the combined therapy group and a mean of 0.66 PDT retreatments performed in the PDT monotherapy group were administered.

• ADVERSE EVENTS: Subretinal hemorrhages are well-known adverse events associated with PDT for PCV. In the PDT monotherapy group, a subretinal or subpigment epithelial hemorrhage, or both, of 1 disc diameter or more developed in 15 eyes (17.7%) within 1 month after the initial treatment; however, this occurred in 3 eyes (4.9%) in the combined therapy group. The incidence of hemorrhages was significantly lower in the combined therapy group ($P = .022$, Fisher exact test). Hemorrhages seriously affected vision in 5 eyes in the PDT monotherapy group and in 1 eye in the combined therapy group. One eye with the combined therapy developed a retinal pigment epithelial tear within 1 month, which did not affect vision. No other serious adverse events were recorded.

DISCUSSION

THE PREVALENCE OF PCV IS HIGH IN PRESUMED EXUDATIVE AMD in Asian individuals,[4–6] and when considering the effective treatment for exudative AMD in this race, better management options for PCV should be explored.

PDT with verteporfin resulted in superior results for treating PCV compared with CNV secondary to AMD in the 1-year visual outcomes in Japanese patients.[9] The results may be satisfactory; however, in this era of anti-VEGF therapy, positive anatomic results such as resolution of fluid resulting from intravitreal bevacizumab also were observed in eyes with PCV,[19,28,29] suggesting that a certain amount of bevacizumab may act directly on the abnormal vasculature in the subretinal pigment epithelial spaces. However, limited efficacy of bevacizumab monotherapy was observed when treating the abnormal vasculature of PCV, and we suggest 2 possible reasons: that an insufficient amount of bevacizumab may reach the subretinal pigment epithelial spaces because of its larger molecular size or the VEGF-independent nature of PCV.[10,19] It seemed important to determine whether there was additional or complimentary efficacy of bevacizumab combined with PDT when treating PCV, especially during a longer follow-up.

In the current study, an additional positive effect of an intravitreal bevacizumab was observed in the visual outcomes through 1 year. During the early treatment period, the efficacy of bevacizumab for improving BCVA was apparent. ANCOVA showed that the combined therapy resulted in maximum improvement in the BCVA at 3 months, which was attributed primarily to rapid resolution of the exudative fluid and fibrin induced by bevacizumab, as we observed previously.[19] The leakage from abnormal vessels was treated effectively through the reduction of VEGF. Moreover, bevacizumab may prevent transient induction of VEGF after PDT[30] and subsequent reaction of vessels.

We also found a significantly lower rate of subretinal or subpigment epithelial hemorrhages, or both, associated with PDT in the combined treatment group. The rate of development of hemorrhage of 1 optic disc diameter within 1 month after PDT monotherapy was 17.7%, which was almost the same as the 19% that we reported previously.[9] However, hemorrhages developed in only 4.9% of the patients in the combined treatment group. The development of subretinal hemorrhages after PDT is a characteristic adverse event after PDT used to treat PCV, and something that physicians want to avoid. In addition to the decreased vascular permeability, the vasoconstrictive effect of bevacizumab[31,32] may result in suppression of hemorrhages. The reduced risk of hemorrhages induced by bevacizumab would encourage ophthalmologists to choose the combined therapy.

For the long-term VA, however, the impact of the combined therapy decreased possibly because of lesion recurrences and atrophic tissue changes related to persistent lesions. Resolution of the original PCV vasculature was observed at a similar rate between the treatments, and the recurrence rates also were similar. This seemed reasonable, because our previous studies showed that bevacizumab monotherapy did not cause regression of the abnormal PCV vasculature, and the resolution of polypoidal lesions may be attributed mainly to PDT alone.[9,10,19] However, analyses elucidating factors associated with a better 12-month VA selected combined therapy as significant in addition to better baseline VA, smaller lesion size, and the absence of PED. The vision in PCV after PDT beyond 1 year is reported to be not as good as within 1 year.[14] During longer follow-up periods, several additional sessions of PDT would be necessary for the recurrences of PCV; that means an increase of risks induced by PDT such as subretinal hemorrhages or ischemic damage of normal choroidal tissue.[33] PDT combined with an anti-VEGF drug can reduce those side effects of PDT. Also, injection of an anti-VEGF drug without PDT is an option for eyes with good vision or intermediate treatments for recurrent fluid or the CNV-like abnormal vasculature that can developed after PDT.[15] Thus, the appropriate combination of an anti-VEGF drug and PDT is important to maintain better VA for the long term.

Recently, Kokame and associates reported the 6-month interim results of monthly injections of ranibizumab (Lucentis; Genentech, South San Francisco, California, USA) in 12 eyes with PCV (PEARL Trial; clinicaltrials.gov identifier, NCT00424710).[34] The results showed that ranibizumab monotherapy improved the mean VA at 6 months by a mean of 7.2 letters and that 2 patients (17%) gained more than 15 letters. That seemed almost the same as the visual results in our combined therapy group at 12 months. In their manuscript, the polypoidal lesions seen on ICGA decreased in 4 eyes (33%) at 6 months, and the authors suggested that the smaller molecular size of ranibizumab compared with bevacizumab and monthly continuous injections may enable the drug to penetrate into the subretinal pigment epithelial space more efficiently. However, it meant difficulties in achieving complete resolution

of polypoidal lesions even after 6 monthly injections of ranibizumab. With the fact that the choroidal vascular networks persisted in all 12 eyes, ranibizumab monotherapy has the potential for continuous risk of recurrences. The pathogenesis of PCV is unknown, but the results suggested that VEGF may not be associated with the development and maintenance of abnormal vasculature of PCV.

The current study was limited because it was retrospective and not a randomized, comparative trial. However, the absence of bias in the choice of the initial treatment and a relatively large number of eyes that had not received any previous treatments compensated for these limitations. We believe the study results offer informative data to clinicians. From the results of the prospective randomized clinical trial comparing the 6-month results among PDT combined with intravitreal ranibizumab, PDT monotherapy, and ranibizumab for PCV (EVEREST Study; clinicaltrials.gov identifier, NCT00674323), it would be helpful to know which treatment should be chosen as the initial therapy, although the differences of efficacy between ranibizumab and bevacizumab remained to be clarified. Furthermore, improved methods to manage PCV are needed to preserve vision over the long term.

THE AUTHORS INDICATE NO FINANCIAL SUPPORT OR FINANCIAL CONFLICT OF INTEREST. INVOLVED IN DESIGN (F.G.) AND conduct (F.G., M.S., M.T.) of study; data collection (F.G., M.S., Y.S.); Analysis and interpretation of the data (F.G., T.W., Y.S.); and Writing (F.G., T.W.), critical revision (M.T., T.W.), and approval (F.G., M.S., M.T.) of the manuscript. The off-label use of bevacizumab and this retrospective study were approved by the Institutional Review Board of Osaka University Hospital, Osaka, Japan. All patients provided written informed consent. The study adhered to the tenets of the Declaration of Helsinki. The authors thank Dr Toshimitsu Hamasaki, Department of Biomedical Statistics, Osaka University Medical School, for performing the statistical analyses.

REFERENCES

1. Spaide RF, Yannuzzi LA, Slakter JS, et al. Indocyanine green videoangiography of idiopathic polypoidal choroidal vasculopathy. Retina 1995;15:100–110.
2. Yannuzzi LA, Ciardella A, Spaide RF, et al. The expanding clinical spectrum of idiopathic polypoidal choroidal vasculopathy. Arch Ophthalmol 1997;115:478–485.
3. Yannuzzi LA, Wong DWK, Storzolini BS, et al. Polypoidal choroidal vasculopathy and neovascularized age-related macular degeneration. Arch Ophthalmol 1999;117:1503–1510.
4. Ciardella AP, Donsoff IM, Huang SJ, et al. Polypoidal choroidal vasculopathy. Surv Ophthalmol 2004;49:25–37.
5. Sho K, Takahashi K, Yamada H, et al. Polypoidal choroidal vasculopathy: incidence, demographic features, and clinical characteristics. Arch Ophthalmol 2003;121:1392–1396.
6. Maruko I, Iida T, Saito M, et al. Clinical characteristics of exudative age-related macular degeneration in Japanese patients. Am J Ophthalmol 2007;144:15–22.
7. Treatment of Age-Related Macular Degeneration with Photodynamic Therapy (TAP) Study Group. Photodynamic therapy of subfoveal choroidal neovascularization in age-related macular degeneration with verteporfin: one-year results of 2 randomized clinical trials—TAP report. Arch Ophthalmol 1999;117:1329–1345.
8. Chan WM, Lam DS, Lai TY, et al. Photodynamic therapy with verteporfin for symptomatic polypoidal choroidal vasculopathy. Ophthalmology 2004;111:1576–1584.
9. Gomi F, Ohji M, Sayanagi K, et al. 1-Year outcomes of photodynamic therapy in age-related macular degeneration and polypoidal choroidal vasculopathy in Japanese patients. Ophthalmology 2008;115:141–146.
10. Gomi F, Tano Y. Polypoidal choroidal vasculopathy and treatments. Curr Opin Ophthalmol 2008;19:208–212.
11. Honda S, Imai H, Yamashiro K, et al. Comparative assessment of photodynamic therapy for typical age-related macular degeneration and polypoidal choroidal vasculopathy: a multicenter study in Hyogo Prefecture, Japan. Ophthalmologica 2009;223:333–338.
12. Sayanagi K, Gomi F, Sawa M, et al. Long-term follow-up of polypoidal choroidal vasculopathy after photodynamic therapy with verteporfin. Graefes Arch Clin Exp Ophthalmol 2007;245:1569–1571.
13. Akaza E, Mori R, Yuzawa M. Long-term results of photodynamic therapy of polypoidal choroidal vasculopathy. Retina 2008;28:717–722.
14. Kurashige Y, Otani A, Sasahara M, et al. Two-year results of photodynamic therapy for polypoidal choroidal vasculopathy. Am J Ophthalmol 2008;146:513–519.
15. Wakabayashi T, Gomi F, Sawa M, et al. Marked vascular changes of polypoidal choroidal vasculopathy after photodynamic therapy. Br J Ophthalmol 2008;92:936–940.
16. Hirami Y, Tsujikawa A, Otani A, et al. Hemorrhagic complications after photodynamic therapy for polypoidal choroidal vasculopathy. Retina 2007;27:335–341.
17. Avery RL, Pieramici DJ, Rabena MD, et al. Intravitreal bevacizumab (Avastin) for neovascular age-related macular degeneration. Ophthalmology 2006;113:363–372.
18. Costa RA, Jorge R, Calucci D, et al. Intravitreal bevacizumab for choroidal neovascularization caused by AMD (IBeNA Study): results of a phase I dose-escalation study. Invest Ophthalmol Vis Sci 2006;47:4569–4578.
19. Gomi F, Sawa M, Sakaguchi H, et al. Efficacy of intravitreal bevacizumab for polypoidal choroidal vasculopathy. Br J Ophthalmol 2008;92:70–73.
20. Lai TY, Chan WM, Liu DT, et al. Intravitreal bevacizumab (Avastin) with or without photodynamic therapy for the treatment of polypoidal choroidal vasculopathy. Br J Ophthalmol 2008;92:661–666.
21. Cho M, Barbazetto IA, Freund KB. Refractory neovascular age-related macular degeneration secondary to polypoidal choroidal vasculopathy. Am J Ophthalmol 2009;148:70–78.
22. Lazic R, Gabric N. Verteporfin therapy and intravitreal bevacizumab combined and alone in choroidal neovascularization due to age-related macular degeneration. Ophthalmology 2007;114:1179–1185.
23. Spaide RF. Rationale for combination therapies for choroidal neovascularization. Am J Ophthalmol 2006;141:149–156.

24. Kaiser PK. Verteporfin photodynamic therapy and anti-angiogenic drugs: potential for combination therapy in exudative age-related macular degeneration. Curr Med Res Opin 2007;23:477–487.
25. Navea A, Mataix J, Desco MC, et al. One-year follow-up of combined customized therapy. Photodynamic therapy and bevacizumab for exudative age-related macular degeneration. Retina 2009;29:13–19.
26. Kaiser PK, Registry of Visudyne AMD Therapy Writing Committee. Verteporfin photodynamic therapy combined with intravitreal bevacizumab for neovascular age-related macular degeneration. Ophthalmology 2009;116:747–755.
27. Akaike H. A new look at statistical model identification. IEEE Trans Automatic Control 1974;19:716–723.
28. Lee SY, Kim JG, Joe SG, et al. The therapeutic effects of bevacizumab in patients with polypoidal choroidal vasculopathy. Korean J Ophthalmol 2008;22:92–99.
29. Song JH, Byeon SH, Lee SC, et al. Short-term safety and efficacy of a single intravitreal bevacizumab injection for the management of polypoidal choroidal vasculopathy. Ophthalmologica 2009;223:85–92.
30. Schmidt-Erfurth U, Schlötzer-Schrehard U, Cursiefen C, et al. Influence of photodynamic therapy on expression of vascular endothelial growth factor (VEGF), VEGF receptor 3, and pigment epithelium-derived factor.Invest Ophthalmol Vis Sci 2003;44:4473–4480.
31. Soliman W, Vinten M, Sander B, et al. Optical coherence tomography and vessel diameter changes after intravitreal bevacizumab in diabetic macular oedema. Acta Ophthalmol 2008;86:365–371.
32. Papadopoulou DN, Mendrinos E, Mangioris G, et al. Intravitreal ranibizumab may induce retinal arteriolar vasoconstriction in patients with neovascular age-related macular degeneration. Ophthalmology 2009;116:1755–1761.
33. Dewi NA, Yuzawa M, Tochigi K, Kawamura A, Mori R. Effects of photodynamic therapy on the choriocapillaris and retinal pigment epithelium in the irradiated area. Jpn J Ophthalmol 2008;52:277–281.
34. Kokame GT, Yeung L, Lai JC. Continuous anti-VEGF treatment with ranibizumab for polypoidal choroidal vasculopathy: 6-month results. Br J Ophthalmol 2010;94:297–301.

Biosketch

Fumi Gomi, MD, is an Associate Professor of the Department of Ophthalmology at the Osaka University Medical School, Japan. She completed her ophthalmology residency at Osaka University Hospital and a fellowship at the Osaka Rosai Hospital in Japan. She received her PhD from Osaka University Graduate School of Medicine in 2001. She currently specializes in macular diseases.

Effect of Cataract in Evaluation of Macular Pigment Optical Density by Autofluorescence Spectrometry

Yuzuru Sasamoto, Fumi Gomi, Miki Sawa, Hirokazu Sakaguchi, Motokazu Tsujikawa and Kohji Nishida

Purpose. To assess the effect of cataract on the evaluation of macular pigment optical density (MPOD) in aged patients.

Methods. MPOD was prospectively measured using autofluorescence spectrometry before and after cataract surgery. The Lens Opacities Classification System III was used to grade the cataracts at baseline.

Results. Forty-five eyes of 41 subjects, who had no ocular disorders or fundus autofluorescence abnormalities except for age-related nuclear cataract, were included. Preoperative MPOD was 0.350 ± 0.117 density unit (DU). Regression analysis showed that a higher nuclear color score correlated with lower MPOD ($t = -2.90$, $P = 0.0063$). The preoperative MPOD prediction formula was MPOD = 0.545 − 0.069 × nuclear color score. A higher nuclear color score correlated significantly with failure to measure the MPOD ($\chi^2 = 5.08$, $P = 0.0242$). The mean postoperative MPOD was 0.600 DU (95% confidence interval [CI], 0.562–0.637), which was significantly ($P < 0.0001$) higher than the preoperative level of 0.350 DU (95% CI, 0.313–0.388). Regression analysis showed that higher preoperative MPOD correlated with higher postoperative MPOD ($t = 2.91$, $P = 0.0061$).

Conclusions. Cataract, especially its nuclear component, affects MPOD measured by autofluorescence spectrometry. Care should be taken when using this method in eyes with age-related macular maculopathy and age-related macular degeneration and in older patients who may develop these diseases. (*Invest Ophthalmol Vis Sci.* 2011;52:927–932) DOI:10.1167/iovs.10-5664

Macular pigment comprises three carotenoids (lutein, zeaxanthin, and mesozeaxanthin)[1–5] and has light-absorbing properties in the 400- to 540-nm range, with maximum absorption at approximately 460 nm.[5–8] In addition, the macular pigment itself has an antioxidative effect.[5,9–13] Thus, macular pigment helps retard some destructive processes in the retina and the retinal pigment epithelium, which may lead to macular diseases such as age-related maculopathy (ARM) and age-related macular degeneration (AMD).

Some investigators have tried to measure the macular pigment to determine its relationship with the development of ARM or AMD.[14–17] Several clinical methods of measuring macular pigment optical density (MPOD) have been used, including heterochromatic flickering photometry (HFP), motion-detection photometry, fundus reflectance spectroscopy, Raman spectrometry, and autofluorescence spectrometry.[18] To date, factors such as sex, aging, race, smoking, and cataract are postulated to affect the density of the macular pigment[15,19–21]; however, the data are not consistent among the published reports.

Cataract absorbs blue light, which damages the retina and may cause development of AMD.[22,23] In addition to visual deterioration, the blue light–absorbing property of cataracts may affect the accuracy of the MPOD measurements. Autofluorescence spectrometry, which uses a two-wavelength method to measure MPOD, acquires fundus autofluorescence (FAF) images obtained at two wavelengths, 488 and 514 nm and then the subtraction of the logarithm of these images creates an MPOD map.[24–27]

Since 488-nm is within the range of blue light, cataracts may reduce the signals in a 488-nm autofluorescence image.[28–31] Thus, when we measure the MPOD in the eyes of elderly people, we should know how cataracts affect the results.

In the present study, we used autofluorescence spectrometry to measure the MPOD in eyes by using autofluorescence spectrometry before and after surgery to determine the effects of cataract.

Methods

Study Population

We conducted a prospective interventional study at Osaka University Hospital from November 2008 to December 2009. The institutional review board approved the study.

Consecutive patients were enrolled who had no ocular disorders, including FAF abnormalities, except for age-related nuclear cataract. Subjects taking supplements containing lutein, zeaxanthin, and/or beta carotene were excluded. The patients underwent standard phacoemulsification and implantation of a yellow-tinted intraocular lens (IOL) (AcrySof SN60WF; Alcon Laboratories, Fort Worth, TX). No complications or adverse events occurred during cataract surgery or the follow-up period. In accordance with the Declaration of Helsinki, all participants provided informed consent before MPOD was measured.

Measurement and Analysis of MPOD

We used modified angiography (Heidelberg Retina Angiograph [HRA], Heidelberg Engineering, Dossenheim, Germany) to measure MPOD in all eyes before and after cataract surgery. The principle of measurement of MPOD with autofluorescence spectrometry with the two-wavelength method has been published.[18,24–27,32] All measurements were performed by two masked orthoptists, who used the same testing device and protocol. Before the study, the reliability of the measurements between these two orthoptists was confirmed as reported previously.[33] MPOD was measured within 1 week before cataract surgery and within 2 weeks after cataract surgery.

From the Department of Ophthalmology, Osaka University Graduate School of Medicine, Osaka, Japan.

Supported in part by Bausch & Lomb Japan, Ltd., Tokyo, Japan.

Submitted for publication April 8, 2010; revised August 16 and October 12, 2010; accepted October 13, 2010.

Disclosure: **Y. Sasamoto**, None; **F. Gomi**, None; **M. Sawa**, None; **H. Sakaguchi**, None; **M. Tsujikawa**, None; **K. Nishida**, None

Corresponding author: Fumi Gomi, Department of Ophthalmology, Osaka University Graduate School of Medicine, 2-2 Yamada-oka, Suita, Osaka 565-0871, Japan; fgomi@ophthal.med.osaka-u.ac.jp.

Before the measurement, sufficient pupil dilation was obtained by instillation of dilating drops containing 0.5% tropicamide and 2.5% phenylephrine. Subjects sat before a table and fixated with the fellow eye on an external light source. If the fellow eye did not have adequate visual acuity (VA) for fixation, the subjects were asked to look straight as much as possible. The modified angiograph was aligned with the subject's eye, and movies were taken with the 488- and 514-nm excitation wavelengths (scan size, 30°); computed mean autofluorescence images were obtained at each wavelength, and the two images were subtracted to calculate the MPOD (expressed as the density unit [DU]). The mean MPOD, averaged along the area of an annulus with a retinal eccentricity of 0.5° (1° circle at the fovea), was selected as the value representing the MPOD. We measured the MPOD two or three times in each eye during each visit and then selected the data with the best-qualified image.[25]

The signal intensities of each 488- and 514-nm autofluorescence image were displayed in gray scale, with levels from 0 to 255. Delori et al.[24] reported the following equation for calculating MPOD, in which K is a constant, and F_p and F_f are the gray level in the perifoveal area (6° circle) and the fovea (0.5° circle), respectively.

$$\text{MPOD} = K\{\log[F_p(488\text{ nm})/F_f(488\text{ nm})]\} - \log[F_p(514\text{ nm})/F_f(514\text{ nm})]$$

To record the components while calculating the MPOD, we manually measured the F_p and F_f in the 488- and 514-nm images before and after surgery in all patients and converted the values into a logarithmic scale referring to the above formula and described the results as the mean (95% CI). The distribution profiles of gray levels of 20 × 20 pixels at the peripheral retina were also obtained, and the skew of the distribution was estimated by calculating the following equation

$$\text{Skew} = [(GL_{5\%} + GL_{95\%})/2 - GL(\text{mode})]/GL(\text{mode})$$

where $GL_{5\%}$ and $GL_{95\%}$ are the 5th and 95th percentiles of the gray level (GL), and GL(mode) is the most frequently occurring gray level. The skew, which is considered to be one of the indexes of random noise of the autofluorescence image, was also described as the mean (95% CI).

Ophthalmic Examination

The clinical examinations included best corrected VA (BCVA) determined with Landolt C charts, intraocular pressure, slit lamp biomicroscopy, and ophthalmoscopy with lens and fundus photographs taken before and after cataract surgery. The slit lamp digital images were used to assess the type and the severity of the lens opacities. Two masked ophthalmologists (YS and FG) graded the nuclear opalescence, nuclear color, and cortical and posterior subcapsular cataracts in each eye based on the Lens Opacities Classification System III (LOCS III).[34]

The nuclear opalescence and color in the observed lens were classified into standards 1 through 6 and scored from 0.1 to 6.9 (ranging from clear or colorless to very opaque or brunescent) by each observer and the average scores were chosen. Eyes with a cortical cataract were graded based on the area of the opacity. We defined eyes with a grade of more than 3.0 (area with opacity within the pupillary area exceeding 20%) as having a cortical cataract. Similarly, eyes with a posterior subcapsular cataract were graded on the basis of the size of the opacity. We defined eyes with a grade of more than 1.0 (obvious opacity at the center of the posterior lens) as having a posterior subcapsular cataract.

Statistical Analysis

Since variations in an individual patient were nearly equivalent to those between patients, all eyes in which the MPOD was measured were included in the analysis, even if both eyes of a patient underwent cataract surgeries. The BCVA was converted to the logarithm of the minimum angle of resolution (logMAR) for the statistical analysis. In comparing the mean logMAR VA and MPOD before and after cataract surgery, the 95% CI was calculated, and a paired t-test was performed.

To estimate the difference in MPOD between subgroups, we analyzed the following parameters by t-test: sex, smoking history, and presence of a cortical cataract and posterior subcapsular cataract. The correlation between the MPOD and age, nuclear opalescence score, nuclear color score, and the logMAR VA, and the correlation between nuclear opalescence or color score and logMAR VA was assessed by calculating Pearson's correlation coefficient (r). Stepwise regression analysis using the Akaike information criterion was performed to determine the variables that affected MPOD before cataract surgery and the difference between MPOD before and after cataract surgery: sex, age, smoking, nuclear opalescence and color score, cortical cataract, posterior subcapsular cataract, and preoperative logMAR VA.[35] When stepwise regression was performed to determine the variables that affected MPOD after cataract surgery, we included sex, age, smoking, postoperative logMAR VA, and preoperative MPOD as explanatory variables. Stepwise regression analysis was also conducted, to determine the variables that correlate with failure to obtain reliable MPOD data.

To estimate the difference in gray levels of the perifoveal area (F_p) and the fovea (F_f) before and after cataract surgery, we performed a paired t-test. The difference in F_p/F_f before and after surgery at 488 and 514 nm was also estimated by paired t-test. Pearson's correlation coefficient (r) was used to determine the correlation between the nuclear color score and the skew index. $P < 0.05$ was considered significant (JMP software version 8.0; SAS Institute Inc., Cary, NC).

Results

Baseline Characteristics and MPOD

A total of 45 eyes of 41 subjects (16 men, 18 eyes; 25 women, 27 eyes) were included. The baseline characteristics of all eyes are shown in Table 1. The mean age ± SD was 71.6 ± 6.7 years. Sixteen patients (18 eyes) were smokers, and 25 (27 eyes) were nonsmokers. The mean ± SD nuclear opalescence and color scores were 2.9 ± 0.9 and 3.0 ± 0.9, respectively, and they correlated very strongly with each other ($r = 0.97$, $P < 0.0001$). The logMAR BCVA (mean ± SD) was 0.39 ± 0.29. The mean preoperative MPOD measured by autofluorescence spectrometry was 0.350 ± 0.117 DU. We could not obtain reliable data (200/225 pixels) in five eyes and excluded them from the preoperative evaluation.

MPOD before cataract surgery is summarized in Table 2. It was significantly reduced, in parallel with the increases in the

Table 1. Baseline Characteristics

Parameter	
Subjects/eyes, *n*	41/45
Sex	
Men/women, *n* subjects	16/25
Men/women, *n* eyes	18/27
Age, mean y ± SD	71.6 ± 6.7
Smokers, *n*	
Yes/no, *n* subjects	16/25
Yes/no, *n* eyes	18/27
Nuclear scores by LOCS III, mean ± SD	
Opalescence	2.9 ± 0.9
Color	3.0 ± 0.9
Cortical cataract, yes/no, *n* eyes	20/25
Posterior subcapsular cataract, yes/no, *n* eyes	13/32
LogMAR VA, mean ± SD	0.394 ± 0.291
Preoperative MPOD measured by autofluorescence spectrometry, DU	0.350 ± 0.117
Subjects with unreliable data, *n*	5

TABLE 2. The MPOD Level before Cataract Surgery

Parameter	MPOD (95% CI) (DU)		*P*
Men/women	0.316 (0.241-0.391) (n = 16)	0.373 (0.333-0.413) (n = 24)	0.1345
Smoking, yes/no	0.322 (0.261-0.383) (n = 15)	0.367 (0.320-0.414) (n = 25)	0.2408
Cortical cataract, yes/no	0.356 (0.296-0.416) (n = 18)	0.345 (0.294-0.397) (n = 22)	0.7781
Posterior subcapsular cataract, yes/no	0.326 (0.219-0.432) (n = 9)	0.357 (0.317-0.398) (n = 31)	0.4782

	Coefficient Correlation (r)	*P*
Age (n = 40)	0.05	0.7570
Nuclear opalescence score by LOCS III (n = 40)	−0.37	0.0177
Nuclear color score by LOCS III (n = 40)	−0.39	0.0142
Preoperative logMAR VA (n = 40)	−0.42	0.0077

nuclear opalescence and color scores and the preoperative logMAR VA (r = −0.37, P = 0.0177; r = −0.39, P = 0.0142; and r = −0.42, P = 0.0077, respectively), although a strong correlation was found between the nuclear opalescence and color scores and the preoperative logMAR VA (r = 0.71, P < 0.0001; r = 0.70, P < 0.0001, respectively). Because these factors were considered to have some correlation with each other, we performed a stepwise regression analysis to ascertain factors that mainly affected MPOD. The analysis showed that a higher nuclear color score was the factor that correlated significantly with lower preoperative MPOD (t = −2.90, P = 0.0063) among variables that included sex, age, smoking, nuclear opalescence and color scores, cortical cataract, posterior subcapsular cataract, and preoperative logMAR VA. The analysis also showed a tendency for MPOD to be higher in the women than in the men (t = 2.01, P = 0.0515). The MPOD prediction formula was MPOD = 0.545 − 0.069 × (nuclear color score). If the nuclear color score increased 1 point, MPOD decreased 0.069 DU.

Stepwise regression analysis also was conducted to determine the factors that were correlated with failure to measure MPOD. A higher nuclear color score correlated significantly with failure to measure the MPOD (χ^2 = 5.08, P = 0.0242). A posterior subcapsular cataract also tended to correlated with failure to measure the MPOD (χ^2 = 3.25, P = 0.0713).

Postoperative MPOD

The mean postoperative logMAR VA was −0.002 (95% CI, −0.038 to 0.034), and it improved significantly compared with the preoperative logMAR VA of 0.394 (95% CI, 0.306-0.481; P < 0.0001).

We could obtain MPOD data in all eyes after cataract surgery. A representative case was shown in Figure 1. The mean postoperative MPOD was 0.600 ± 0.124 DU (95% CI, 0.562-0.637). The postoperative MPOD was significantly higher than the preoperative level of 0.350 ± 0.117 DU (95% CI, 0.313-0.388; P < 0.0001). Postoperative MPOD correlated positively with the preoperative level (r = 0.43, P = 0.0058; Fig. 2).

MPOD data after cataract surgery are summarized in Table 3. The MPOD tended to be higher in the women (0.626 [95% CI, 0.582-0.670]) than in the men (0.559 [95%

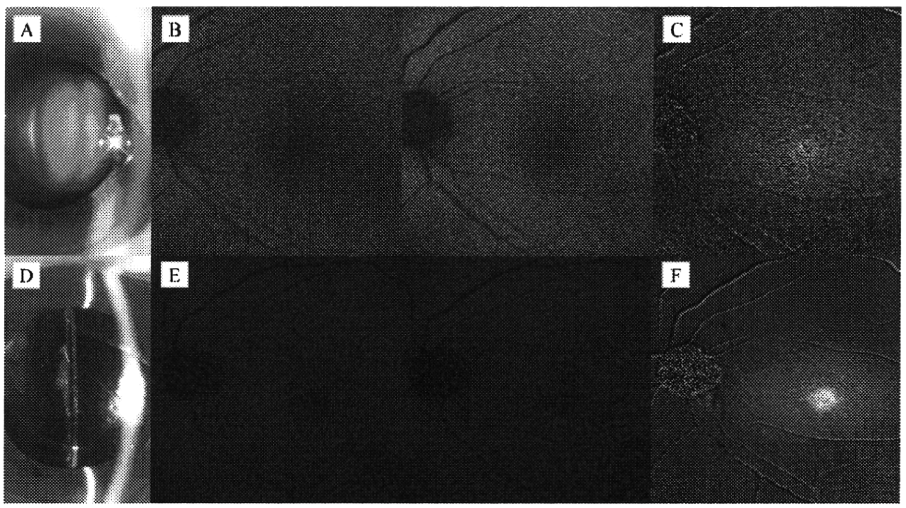

FIGURE 1. Pre- and postoperative images from an eye of a 71-year-old woman. (**A**) Preoperative color of the cataract nuclear was scored as 4.2 and the nuclear opalescence score as 4.0. (**B**) Fundus autofluorescence images captured at the 488-nm (*left*) and 514-nm (*right*) wavelengths before surgery. The sensitivity of the detector was set relatively high, and random noise was seen in both images. The macular pigment blocked more signals from the macula in the 488-nm image. (**C**) The subtraction of the logarithm of these images creates an MPOD map. Preoperative MPOD was 0.29 DU. (**D**) A yellow-tinted IOL implanted during the surgery. (**E**) Postoperative fundus autofluorescence images captured at 488-nm (*left*) and 514-nm (*right*) wavelengths. The proper setting of the sensitivity of the detector led to less random noise. (**F**) Postoperative MPOD improved to 0.66 DU.

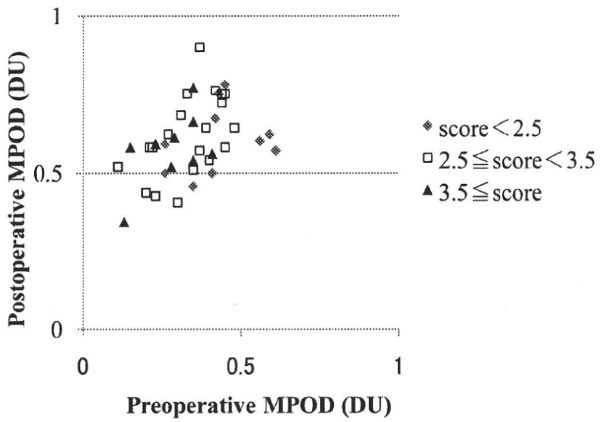

FIGURE 2. Preoperative and postoperative MPODs by the nuclear color score of the lens (n = 40). The shape of the data points represents the nuclear color scores shown at *right*. The postoperative MPOD correlated positively with the preoperative level (r = 0.43, P = 0.0058).

CI, 0.493-0.626]; P = 0.0758). In addition, it tended to be in proportion to age (r = 0.29, P = 0.0547). The postoperative level correlated positively with the preoperative one (r = 0.43, P = 0.0058). We conducted a stepwise regression analysis in which the model included sex, age, smoking, postoperative logMAR acuity, and preoperative MPOD as explanatory variables and postoperative MPOD as a response. The analysis showed that higher preoperative MPOD correlated with higher postoperative MPOD (t = 2.91, P = 0.0061).

Difference in MPOD before and after Surgery

Simple regression analysis revealed that eyes with lower preoperative MPOD and a higher nuclear color score correlated with the larger difference in MPOD before and after cataract surgery (r = −0.54, P = 0.0001 and r = 0.36, P = 0.0157, respectively). After conducting a stepwise regression analysis, we found lower preoperative MPOD and no presence of posterior subcapsular cataract correlated with a larger difference in MPOD (t = −4.51, P < 0.0001; t = −2.18, P = 0.0355, respectively).

Gray Levels and Skew before and after Surgery

Gray level at the perifoveal region (F_p) and the fovea (F_f) and their ratio (F_p/F_f) before and after cataract surgery presented in logarithmic scale are summarized in Table 4. F_p before and after surgery did not change significantly at both 488 and 514 nm (P = 0.4167, P = 0.6848, respectively). F_f at 514 nm also did not show a significant change (P = 0.3808), but F_f at 488 nm significantly decreased after surgery (P = 0.0136). In addition, the increase in F_p/F_f after surgery at 488 nm was significantly higher than that at 514 nm: 0.19 (95% CI, 0.16-0.22) and 0.07 (95% CI, 0.05-0.09), respectively (P < 0.0001).

The skew at the peripheral retina is also shown in Table 4. It was significantly higher before surgery than after in both the 488- and the 514-nm images (P = 0.0001 and P < 0.0001, respectively). Statistical analysis showed that the higher skew index at 488 nm correlated moderately with higher nuclear color score (r = 0.43, P = 0.0028), but skew at 514 nm did not correlate with the nuclear color score (r = −0.02, P = 0.8995).

Discussion

We used autofluorescence spectrometry to measure MPOD in eyes with age-related cataract, before and after cataract surgery, and observed the significant increase in MPOD after cataract surgery. Mean MPOD was 0.350 DU (95% CI, 0.313-0.388) before surgery and 0.600 DU (95% CI, 0.562-0.637) after surgery. Considering the result from the previous report that the intensity of macular pigment is stable without intervention,[36] the increased MPOD observed after cataract surgery must be artifactual. Therefore, we examined the factors that correlated with MPOD.

MPOD significantly increased after the cataractous lenses were removed and replaced with yellow IOLs, the color of which was similar to the lens color in subjects in the third decade of life. Preoperative MPOD tended to be lower when the nuclear opalescence and color scores were high, although there was no correlation between preoperative MPOD and cortical cataracts or posterior subcapsular cataracts. As expected, the nuclear opalescence score and the nuclear color score correlated very strongly (r = 0.97, P < 0.0001), but stepwise regression analysis showed that the nuclear color score was the most significant factor that affected preoperative MPOD (t = −2.90, P = 0.0063). In addition, we found in a simple regression analysis that lower preoperative MPOD and a higher nuclear color score correlated with a larger difference in MPOD. From these results, we concluded that the lower MPOD in the eyes with cataract was, to some degree, due to the yellower lenses.

As a reason for MPOD reduction by the presence of cataract, first, we hypothesized that the lens yellowing might reduce the autofluorescence level in 488-nm (blue) wavelength directly because yellow absorbs blue. However, as the lens yellowing reduced the autofluorescence at the perifoveal area and the fovea equally, it seemed not to affect the final MPOD in the equation used to calculate it.[24] Then, we examined gray levels in all images and also the skew condition. Finally, we reached the following conclusions: Excitation and emission signals are scattered by cataractous lenses, and excitation signals are partially absorbed by yellow lenses. Hence, to obtain an image bright enough to evaluate MPOD, we had to make the

TABLE 3. The MPOD Level after Cataract Surgery

	MPOD (95% CI) (DU)		P
Men/women	0.559 (0.493-0.626) (n = 18)	0.626 (0.582-0.670) (n = 27)	0.0758
Smoking, yes/no	0.573 (0.507-0.638) (n = 18)	0.617 (0.571-0.664) (n = 27)	0.2407
	Coefficient Correlation (r)		**P**
Age (n = 45)	0.29		0.0547
Postoperative logMAR VA (n = 45)	0.18		0.2313
Preoperative MPOD (n = 40)	0.43		0.0058

TABLE 4. Grey Levels before and after Cataract Surgery

	F_p	F_f	F_p/F_f	Skew (95% CI)
Before surgery				
488-nm	1.33 (1.24-1.42)	0.96 (0.86-1.07)	0.37 (0.33-0.40)	0.28 (0.19-0.36)
514-nm	1.43 (1.34-1.52)	1.22 (1.12-1.31)	0.21 (0.19-0.23)	0.26 (0.18-0.33)
After surgery				
488-nm	1.39 (1.29-1.50)	0.84 (0.72-0.96)	0.56 (0.53-0.59)	0.10 (0.06-0.14)
514-nm	1.48 (1.37-1.58)	1.19 (1.0-1.31)	0.28 (0.26-0.30)	0.10 (0.07-0.14)

Data are expressed as the gray level (95% CI).

sensitivity of the detector high in the cataractous eyes, and this adjustment resulted in higher reflectivity, as seen in Figure 1. As a result, F_p before surgery was at almost the same level after surgery. However, the skew index, which substitutes for random noise, was higher before surgery than after surgery, because high sensitivity induced high levels. This result made the F_f falsely high compared with the F_p before surgery, especially at 488 nm, because foveal signals in 488 nm are small due to the macular pigment and are easily affected by the random noise. Consequently, the increase in F_p/F_f after surgery at 488 nm was significantly higher than that at 514 nm and led to the decrease in MPOD before surgery. The statistical results, which showed a positive correlation between the skew and nuclear color score in the 488-nm wavelength images but not in the 514-nm wavelength images, may indicate that lens yellowing increases the random noise of the autofluorescence image, especially at 488 nm and, as a result, decrease the MPOD. Of course, we might consider other effects such as autofluorescence of the lens. However, as mentioned by Delori et al.,[24] its effect on the MPOD measurement should be very small.

Despite no other ocular diseases apart from cataracts, we could not obtain reliable MPOD measurements in five (11%) eyes by autofluorescence spectrometry. Such a limitation in measuring MPOD in cataractous eyes is a weak point of this method. In eyes with a higher nuclear color score or a posterior subcapsular cataract, there was a tendency toward failure to measure the MPOD. This problem may have occurred because the yellowing of the lens and the dense opacity of the posterior capsule blocked the signals from the fundus, and we could not obtain sufficient effective pixels (200/225 pixels). Also, we found that the absence of posterior subcapsular cataracts correlated with the larger difference in MPOD. The effect of posterior subcapsular cataracts on MPOD remains to be determined.

During cataract surgery, a yellow IOL, the color of which was similar to the lens color in subjects in the third decade of life, was implanted in all patients, and postoperative MPOD increased significantly compared with the preoperative level, although they correlated significantly. The postoperative MPOD may be considered to be close to the true level. Of interest, our study showed that postoperative MPOD in the women tended to be higher than that in the men. The higher MPOD in older women may be one reason that explains the lower rate of progressing AMD in Japanese women, although Caucasian women have more risk of the disease.[37,38] Increasing age is the other factor that tended to be associated with a higher postoperative MPOD, although the age range of this study population was relatively narrow. Elderly people who do not develop AMD or other fundus diseases may have higher MPOD. Because it remains controversial whether MPOD differs by sex and age,[17,21,39,40] further studies are needed.

Our findings do not replicate the results of Ciulla et al.[41] and Nolan et al.,[42] who measured MPOD before and after cataract surgery using HFP. They reported no significant differences between the two time points just before and after cataract surgery. Differences between the methods may chiefly explain this discrepancy, although there may be population-based differences contributed by race and the LOCS grade of the cataracts.

In conclusion, our data suggest that cataracts affect the measurement of MPOD by autofluorescence spectrometry, probably as a result of the high setting of the detector's sensitivity. Nuclear cataract seemed to associate with this high-sensitivity setting, producing a random noise especially in 488-nm wavelength images. Care should be taken when evaluating MPOD using this method in eyes with age-related macular maculopathy and macular degeneration and in patients who are old enough to develop these diseases. More quantitative and higher quality methods of averaging the reflectivity may yield a normalized autofluorescence image in which the effect of cataract is excluded and may allow more precise evaluation of MPOD.

Acknowledgments

The authors thank Thomas Fendrich (Heidelberg Engineering, Dossenheim, Germany) for pertinent and helpful advice.

References

1. Handelman GJ, Dratz EA, Reay CC, van Kuijk JG. Carotenoids in the human macula and whole retina. *Invest Ophthalmol Vis Sci.* 1988;29:850-855.
2. Bone RA, Landrum JT, Tarsis SL. Preliminary identification of the human macular pigment. *Vision Res.* 1985;25:1531-1535.
3. Bone RA, Landrum JT, Friedes LM, et al. Distribution of lutein and zeaxanthin stereoisomers in the human retina. *Exp Eye Res.* 1997; 64:211-218.
4. Bone RA, Landrum JT, Hime GW, Cains A, Zamor J. Stereochemistry of the human macular carotenoids. *Invest Ophthalmol Vis Sci.* 1993;34:2033-2040.
5. Snodderly DM, Auran JD, Delori FC. The macular pigment, II: spatial distribution in primate retinas. *Invest Ophthalmol Vis Sci.* 1984;25:674-685.
6. Snodderly DM, Brown PK, Delori FC, Auran JD. The macular pigment, I: absorbance spectra, localization, and discrimination from other yellow pigments in primate retinas. *Invest Ophthalmol Vis Sci.* 1984;25:660-673.
7. Bone RA, Landrum JT, Cains A. Optical density spectra of the macular pigment in vivo and in vitro. *Vision Res.* 1992;32:105-110.
8. Junghans A, Sies H, Stahl W. Macular pigments lutein and zeaxanthin as blue light filters studied in liposomes. *Arch Biochem Biophys.* 2001;391:160-164.
9. Beatty S, Koh H, Phil M, Henson D, Boulton M. The role of oxidative stress in the pathogenesis of age-related macular degeneration. *Surv Ophthalmol.* 2000;45:115-134.
10. Kirschfeld K. Carotenoid pigments: their possible role in protecting against photooxidation in eyes and photoreceptor cells. *Proc R Soc Lond B Biol Sci.* 1982;216:71-85.
11. Beatty S, Boulton M, Henson D, Koh HH, Murray IJ. Macular pigment and age related macular degeneration. *Br J Ophthalmol.* 1999;83:867-877.

12. Landrum JT, Bone RA, Kilburn MD. The macular pigment: a possible role in protection from age-related macular degeneration. *Adv Pharmacol.* 1997;38:537–556.
13. Khachik F, Bernstein PS, Garland DL. Identification of lutein and zeaxanthin oxidation products in human and monkey retinas. *Invest Ophthalmol Vis Sci.* 1997;38:1802–1811.
14. LaRowe TL, Mares JA, Snodderly DM, Klein ML, Wooten BR, Chappell R. Macular pigment density and age-related maculopathy in the carotenoids in Age-Related Eye Disease Study: an ancillary study of the women's health initiative. *Ophthalmology.* 2008;115:876–883, e871.
15. Nolan JM, Stack J, O'Donovan O, Loane E, Beatty S. Risk factors for age-related maculopathy are associated with a relative lack of macular pigment. *Exp Eye Res.* 2007;84:61–74.
16. Obana A, Hiramitsu T, Gohto Y, et al. Macular carotenoid levels of normal subjects and age-related maculopathy patients in a Japanese population. *Ophthalmology.* 2008;115:147–157.
17. Jahn C, Wustemeyer H, Brinkmann C, Trautmann S, Mossner A, Wolf S. Macular pigment density in age-related maculopathy. *Graefes Arch Clin Exp Ophthalmol.* 2005;243:222–227.
18. Leung IY. Macular pigment: new clinical methods of detection and the role of carotenoids in age-related macular degeneration. *Optometry.* 2008;79:266–272.
19. Hammond BR Jr. Caruso-Avery M. Macular pigment optical density in a Southwestern sample. *Invest Ophthalmol Vis Sci.* 2000;41:1492–1497.
20. Wolf-Schnurrbusch UE, Roosli N, Weyermann E, Heldner MR, Hohne K, Wolf S. Ethnic differences in macular pigment density and distribution. *Invest Ophthalmol Vis Sci.* 2007;48:3783–3787.
21. Iannaccone A, Mura M, Gallaher KT, et al. Macular pigment optical density in the elderly: findings in a large biracial midsouth population sample. *Invest Ophthalmol Vis Sci.* 2007;48:1458–1465.
22. Gaillard ER, Zheng L, Merriam JC, Dillon J. Age-related changes in the absorption characteristics of the primate lens. *Invest Ophthalmol Vis Sci.* 2000;41:1454–1459.
23. Dillon J, Zheng L, Merriam JC, Gaillard ER. Transmission of light to the aging human retina: possible implications for age related macular degeneration. *Exp Eye Res.* 2004;79:753–759.
24. Delori FC, Goger DG, Hammond BR, Snodderly DM, Burns SA. Macular pigment density measured by autofluorescence spectrometry: comparison with reflectometry and heterochromatic flicker photometry. *J Opt Soc Am A Opt Image Sci Vis.* 2001;18:1212–1230.
25. Delori FC. Autofluorescence method to measure macular pigment optical densities fluorometry and autofluorescence imaging. *Arch Biochem Biophys.* 2004;430:156–162.
26. Liew SH, Gilbert CE, Spector TD, et al. Heritability of macular pigment: a twin study. *Invest Ophthalmol Vis Sci.* 2005;46:4430–4436.
27. Wustemeyer H, Jahn C, Nestler A, Barth T, Wolf S. A new instrument for the quantification of macular pigment density: first results in patients with AMD and healthy subjects. *Graefes Arch Clin Exp Ophthalmol.* 2002;240:666–671.
28. van den Berg TJ, Felius J. Relationship between spectral transmittance and slit lamp color of human lenses. *Invest Ophthalmol Vis Sci.* 1995;36:322–329.
29. Boettner EA, Reimer WJ. Transmission of the ocular media. *Invest Ophthalmol Vis Sci.* 1962;1:776–783.
30. Terada H. Spectra transmittance of normal human crystalline lens (in Japanese). *Nippon Ketsueki Gakkai Zasshi.* 1994;98:1101–1108.
31. Algvere PV, Torstensson PA, Tengroth BM. Light transmittance of ocular media in living rabbit eyes. *Invest Ophthalmol Vis Sci.* 1993;34:349–354.
32. Trieschmann M, Heimes B, Hense HW, Pauleikhoff D. Macular pigment optical density measurement in autofluorescence imaging: comparison of one- and two-wavelength methods. *Graefes Arch Clin Exp Ophthalmol.* 2006;244:1565–1574.
33. Sasamoto Y, Gomi F, Sawa M, Tsujikawa M, Hamasaki T. Macular pigment optical density in central serous chorioretinopathy. *Invest Ophthalmol Vis Sci.* 51:5219–5225.
34. Chylack LT Jr, Wolfe JK, Singer DM, et al. The Lens Opacities Classification System III. The Longitudinal Study of Cataract Study Group. *Arch Ophthalmol.* 1993;111:831–836.
35. Akaike H. A new look at the statistical model identification. *IEEE Trans Automat Cont.* 1974;19:716–723.
36. Nolan JM, Stack J, Mellerio J, et al. Monthly consistency of macular pigment optical density and serum concentrations of lutein and zeaxanthin. *Curr Eye Res.* 2006;31:199–213.
37. Yasuda M, Kiyohara Y, Hata Y, et al. Nine-year incidence and risk factors for age-related macular degeneration in a defined Japanese population the Hisayama study. *Ophthalmology.* 2009;116:2135–2140.
38. Kawasaki R, Wang JJ, Ji GJ, et al. Prevalence and risk factors for age-related macular degeneration in an adult Japanese population: the Funagata study. *Ophthalmology.* 2008;115:1376–1381, e1371–1372.
39. Wustemeyer H, Moessner A, Jahn C, Wolf S. Macular pigment density in healthy subjects quantified with a modified confocal scanning laser ophthalmoscope. *Graefes Arch Clin Exp Ophthalmol.* 2003;241:647–651.
40. Ciulla TA, Hammond BR Jr. Macular pigment density and aging, assessed in the normal elderly and those with cataracts and age-related macular degeneration. *Am J Ophthalmol.* 2004;138:582–587.
41. Ciulla TA, Hammond BR Jr, Yung CW, Pratt LM. Macular pigment optical density before and after cataract extraction. *Invest Ophthalmol Vis Sci.* 2001;42:1338–1341.
42. Nolan JM, O'Reilly P, Loughman J, et al. Augmentation of macular pigment following implantation of blue light-filtering intraocular lenses at the time of cataract surgery. *Invest Ophthalmol Vis Sci.* 2009;50:4777–4785.

in the tear fluid did not appear to be correlated with those in the serum.

Comments

We found that the tear fluid of healthy adults contained both sCD14 and LBP. Although the concentrations of these proteins in tear fluid were substantially lower than those in serum from the same individuals, our previous in vitro experiments indicate that the amounts of sCD14 and LBP detected in tear fluid are sufficient to exert maximal effects on chemokine and adhesion molecule expression by corneal fibroblasts in the presence of LPS. The presence of these proteins in tear fluid may thus enhance the perception of LPS by corneal fibroblasts in vivo. Both sCD14 and LBP were previously detected in human reflex tears stimulated by onion vapor.[5] The concentrations of sCD14 in reflex tears were similar to those determined in the present study for basal tears, but the concentrations of LBP were lower in reflex tears than in basal tears. As the lacrimal gland contains more CD14 than LBP,[5] the difference in the LBP concentration between basal and reflex tears might suggest that LBP has additional sources such as the corneal epithelium. Our results highlight the importance of tear fluid in the defense of the cornea against microorganisms. Given that the levels of sCD14 and LBP in tear fluid may be affected by inflammation and are potential novel diagnostic markers for certain diseases, the concentrations of these proteins in tear fluid from individuals with various ocular surface disorders, including allergy, infection, and dry eye, warrant further investigation.

Acknowledgments. This work was supported by a Grant-in-Aid for Scientific Research (KAKENHI, no. 14571674) from the Ministry of Education, Culture, Sports, Science and Technology of Japan. The manuscript was edited by Keith W. Brocklehurst, Ph.D., a professional science editor.

Keywords: innate immunity, lipopolysaccharide, LPS-binding protein, soluble CD14, tear fluid

Ken Fukuda, Naoki Kumagai, and Teruo Nishida
Department of Ophthalmology, Yamaguchi University Graduate School of Medicine, Ube, Yamaguchi, Japan

Received: June 30, 2009 / Accepted: December 28, 2009
Correspondence to: Ken Fukuda, Department of Ophthalmology, Yamaguchi University Graduate School of Medicine, 1-1-1 Minami-Kogushi, Ube, Yamaguchi 755-8505, Japan
e-mail: k.fukuda@yamaguchi-u.ac.jp

DOI 10.1007/s10384-009-0787-z

References

1. Kumagai N, Fukuda K, Fujitsu Y, et al. Lipopolysaccharide-induced expression of intercellular adhesion molecule-1 and chemokines in cultured human corneal fibroblasts. Invest Ophthalmol Vis Sci 2005;46:114–120.
2. Bas S, Gauthier BR, Spenato U, et al. CD14 is an acute-phase protein. J Immunol 2004;172:4470–4479.
3. Gallay P, Barras C, Tobias PS, et al. Lipopolysaccharide (LPS)-binding protein in human serum determines the tumor necrosis factor response of monocytes to LPS. J Infect Dis 1994;170:1319–1322.
4. Fukuda K, Kumagai N, Yamamoto K, et al. Potentiation of lipopolysaccharide-induced chemokine and adhesion molecule expression in corneal fibroblasts by soluble CD14 or LPS-binding protein. Invest Ophthalmol Vis Sci. 2005;46:3095–3101.
5. Blais DR, Vascotto SG, Griffith M, Altosaar I. LBP and CD14 secreted in tears by the lacrimal glands modulate the LPS response of corneal epithelial cells. Invest Ophthalmol Vis Sci 2005;46:4235–4244.

Vascular Endothelial Growth Factor Concentrations in Aqueous Humor Before and After Subconjunctival Injection of Bevacizumab for Neovascular Glaucoma

Neovascular glaucoma (NVG) is a severe complication of proliferative diabetic retinopathy (PDR), central retinal vein occlusion, and other ischemic retinal vascular diseases. Vascular endothelial growth factor (VEGF) is an important component of neovascular formation.[1] Recently, the treatment of NVG with intravitreal injections of anti-VEGF antibody has been reported to cause regression of iris neovascularization[2] and reduction of VEGF concentrations in the aqueous humor.[3] At the same time, complications due to the intravitreal method of administration have also been reported.[4] We herein report subconjunctival injection of bevacizumab (Avastin; Roche, Basel, Switzerland) as an alternative, safer method of administering NVG and describe VEGF concentrations in the aqueous humor both pre- and posttreatment.

Method and Results

The present study was approved by the Institutional Review Board of the Kagawa University Hospital, Kagawa, Japan. Signed informed consent was obtained from all patients.

Subconjunctival injection of 1.25 mg (0.05 ml) bevacizumab was performed in seven eyes of seven patients with NVG secondary to PDR. The bevacizumab was injected as preoperative adjunctive therapy before trabeculectomy in all eyes. Aqueous humor samples were obtained just before the subconjunctival injection of bevacizumab and during trabeculectomy, performed 4–7 days after the injection. Free VEGF concentrations in the aqueous humor were measured with an enzyme-linked immunosorbent assay. The aqueous humor was also sampled during cataract operations from three eyes of three patients with no other ocular diseases, as a control group.

Patient characteristics and the main outcomes are summarized in Table 1. The limit of detection for VEGF was

Table 1. Patient characteristics and clinical data before and after subconjunctival injection of bevacizumab

Case no.	Age (years)	Sex	Previous surgical procedure	IOP before injection (mmHg)	VEGF concentration in aqueous humor (pg/ml)	
					Before injection	After injection (days)
1	59	Male	PRP, PEA+IOL+VIT	22	<31	<31 (7)
2	67	Male	PRP	22	93.1	<31 (5)
3	59	Female	PRP, PEA+IOL+VIT	36	478	127 (4)
4	61	Female	PRP[a]	41	4980	1178 (5)
5	50	Male	PRP	62	6650	868 (6)
6	72	Male	PRP, PEA+IOL	45	11200	1040 (5)
7	63	Female	PRP[a]	76	26400	7530 (4)

IOP, intraocular pressure; VEGF, vascular endothelial growth factor; PRP, panretinal photocoagulation; PEA, phacoemulsification aspiration; IOL, intraocular lens implantation; VIT, vitrectomy.
[a]After bevacizumab injection.

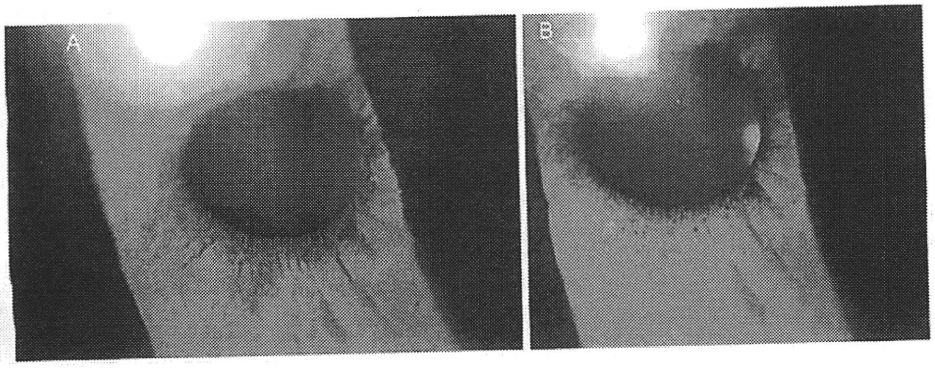

Figure 1A, B. Case 5. See also Table 1. **A** Iris neovascularization prior to subconjunctival injection. Marked neovascularization is seen between the 2 and 8 o'clock positions from the pupillary zone to the parenchyma of the iris. **B** Iris neovascularization following subconjunctival injection. The neovascularization that was seen prior to the injection has regressed.

31 pg/ml. VEGF concentrations in aqueous humor ranged from <31 pg/ml to 26 400 pg/ml before the subconjunctival injection of bevacizumab, and decreased to <31–7530 pg/ml after bevacizumab administration. Concentrations in the control group ranged from <31 pg/ml to 131 pg/ml. Regression of iris neovascularization decreased, except in two eyes, following subconjunctival injection of bevacizumab (Fig. 1). In two cases treated with PRP after a bevacizumab injection (cases 4 and 7; Table 1), the subconjunctival injection did not result in the desired regression of iris neovascularization and an additional intravitreal injection was performed.

In all eyes, bleeding during trabeculectomy was minimal and postoperative hyphema following trabeculectomy was not observed. Systemic or local complications were not observed in any of the cases.

Comment

In the present study, treatment of NVG with subconjunctival injection of bevacizumab resulted in a decreased VEGF concentration in all eyes. We also confirmed that regression of iris neovascularization could be accomplished with this treatment. However, the efficacy of subconjunctival injection was limited in patients in whom high intraocular VEGF concentrations indicated highly active NVG. VEGF concentrations in the aqueous humor of patients not receiving panretinal photocoagulation treatment may be high. Given the findings of Sawada et al.[3] regarding the efficacy of intravitreal injection of bevacizumab for the treatment of PDR, intravitreal injection appears to reduce VEGF concentrations in the aqueous humor more effectively than subconjunctival injection. In NVG cases with relatively low VEGF concentrations, however, the possibility of an overdose of bevacizumab when it is injected into the vitreous cavity cannot be ruled out.

Furthermore, although the incidence is small, severe complications from the intravitreal injection of bevacizumab, such as endophthalmitis or lens injury, have been reported.[4]

Nomoto et al.[5] reported that a minimal amount of bevacizumab could be detected in the iris and ciliary body in rabbits after subconjunctival injection of bevacizumab. Thus, this treatment is likely to result in suppression of NVG. How to select patients for whom subconjunctival injection of bevacizumab will prove helpful is a problem that requires further investigation.

Keywords: bevacizumab, neovascular glaucoma, subconjunctival injection, vascular endothelial growth factor

Masanori Mizote, Tetsuya Baba, Kazuyuki Hirooka, Hidetaka Yamaji, and Fumio Shiraga
Department of Ophthalmology, Kagawa University Faculty of Medicine, Miki, Kagawa, Japan

Jpn J Ophthalmol
Vol 54: 239–254, 2010

Received: July 7, 2009 / Accepted: December 9, 2009
Correspondence to: Masanori Mizote, Department of Ophthalmology, Kagawa University Faculty of Medicine, 1750-1 Ikenobe, Miki, Kagawa 761-0793, Japan
e-mail: m.mizote@med.kagawa-u.ac.jp

DOI 10.1007/s10384-009-0788-y

References

1. Aiello LP, Avery RL, Arrigg PG, et al. Vascular endothelial growth factor in ocular fluid of patients with diabetic retinopathy and other retinal disorders. N Engl J Med 1994;331:1480–1487.
2. Oshima Y, Sakaguchi H, Gomi F, Tano Y. Regression of iris neovascularization after intravitreal injection of bevacizumab in patients with proliferative diabetic retinopathy. Am J Ophthalmol 2006;142: 155–158.
3. Sawada O, Kawamura H, Kakinoki M, Sawada T, Ohji M. Vascular endothelial growth factor in aqueous humor before and after intravitreal injection of bevacizumab in eyes with diabetic retinopathy. Arch Ophthalmol 2007;125:1363–1366.
4. Fung AE, Rosenfeld PJ, Reichel E The international intravitreal bevacizumab safety survey: using the interest to assess drug safety worldwide. Br J Ophthalmol 2006;90:1344–1349.
5. Nomoto H, Shiraga F, Kuno N, et al. Pharmacokinetics of bevacizumab after topical, subconjunctival and intravitreal administration in rabbits. Invest Ophthalmol Vis Sci 2009;50:4807–4813.

Conjunctival Nevus-like Lesions Originating from a Sclerotomy Site After 23-Gauge Transconjunctival Sutureless Vitrectomy

Since transconjunctival sutureless vitrectomy (TSV) was first developed by Fujii et al.,[1] 25-gauge and 23-gauge TSV have been widely used to treat various vitreoretinal diseases because of its advantages of a shorter surgical time and faster recovery. However, questions have arisen regarding the self-sealing characteristics in some cases of postoperative hypotony.[2] We report bilateral nevus-like lesions originating from sclerotomy sites after bilateral 23-gauge TSV.

Case Report

A 51-year-old woman with diabetes mellitus presented with sudden decreased bilateral visual acuity. Best-corrected visual acuity was hand motion OD and 20/400 OS. Biomicroscopic examination results of the anterior segment was normal except for bilateral cataracts. Fundus examination showed vitreous hemorrhage OU. Thus, combined phacoemulsification and 23-gauge TSV (DORC, Zuidland, Holland) were carried out in each eye, 1 week apart. Vitreous base dissection was done under scleral depression. As sclerotomy site leakage was found during the surgery in both eyes, releasable suturing with 8-0 polyamide (Monosof, Syneture, Covidien, Mansfield, MA, USA) was performed at all sclerotomy sites.[3] All of the sutures were released on slit-lamp the day after each surgery. Each wound was evaluated for leakage by a Seidel test at the postoperative follow-up. Intraocular pressure was maintained at 10 mmHg or more, and there were no postoperative complications such as sclerotomy leakage or choroidal detachment.

At 1 month after surgery, conjunctival nevus-like lesions were found in all of the sclerotomy sites in both eyes (Fig. 1A, B).

Three months after surgery, an excisional biopsy was performed under topical anesthesia to resolve cosmetic problems and to rule out melanoma. Conjunctival excision, including of the underlying Tenon's capsule, was carried out in the inferotemporal quadrant of the right eye. As much pigment as possible was removed from the episcleral bed. Then, the amniotic membrane was laid on the episcleral bed with the basement membrane side down and sutured with 10-0 nylon interrupted sutures.

Light microscopic examination of the excised tissue showed nonkeratinizing squamous epithelium and substantia propria of the conjunctiva (Fig. 2A). Infiltration of abundant dark brownish melanophages, macrophages that have ingested melanin pigments in the substantia propria, was observed at higher magnification. Scattered, finely granular, melanin pigmentation surrounding the melanophages was also noted (Fig. 2B). Neither nevus cells nor melanoma cells were observed in the sample.

Six weeks after the conjunctival excision, a pigmented lesion remained in the right inferotemporal site.

Comments

We speculate that melanin was discharged from the sclerotomy sites. First, there was no preexisting conjunctival nevus-like lesion, and the lesion occurred exactly at the three sclerotomy sites in both eyes postoperatively. Second, the light microscopic examination revealed neither nevus cells nor melanoma cells. Smiddy et al.[4] reported similar findings after 20-gauge vitrectomy, but they presumed that the source of melanin was ruptured uveal cells caused by extensive cryotherapy, different from the present case. Vitreous base dissection is one risk factor for sclerotomy leakage requiring suture placement after 23-gauge TSV.[5] The releasable suture technique was developed to prevent incompetent wound closure during the operation and has proved effective in preventing postoperative hypotony.[3] However, it cannot prevent undetectable leakage from sclerotomy sites, in particular, the dispersion of melanin pigments in our case. To our knowledge, this complication has not been reported before and we add this case to possible complications of 23-gauge TSV in patients at risk for vitreous base dissection. Preoperative warning of the possibility of such a complication and meticulous postoperative ante-

Neuroprotection against Retinal Ischemia–Reperfusion Injury by Blocking the Angiotensin II Type 1 Receptor

Kouki Fukuda,[1] *Kazuyuki Hirooka,*[1] *Masanori Mizote,*[1] *Takehiro Nakamura,*[2] *Toshifumi Itano,*[2] *and Fumio Shiraga*[1]

Purpose. To investigate the effects of an angiotensin-converting enzyme (ACE) inhibitor and an angiotensin II antagonist against retinal ischemia-reperfusion injury in the rat retina.

Methods. Retinal ischemia was induced by increasing intraocular pressure to 130 mm Hg. Rats were treated with an ACE inhibitor (captopril), an angiotensin II type 1 receptor (AT1-R) antagonist (candesartan), an AT2-R antagonist (PD123319), bradykinin, or a bradykinin B2 receptor antagonist (icatibant). At 7 days after the ischemia, retinal damage was evaluated. Immunohistochemistry and image analysis were used to measure changes in the levels of reactive oxygen species (ROS) and the localization of AT1-R. Dark-adapted full-field electroretinography (ERG) was also performed.

Results. Pretreatment with captopril or candesartan significantly inhibited the ischemic injury of the inner retina. However, PD123319, bradykinin, or icatibant did not reduce the ischemic damage. In control retinas, retinal vessels were positive for AT1-R. In contrast, 12 hours after ischemia, immunohistochemical analysis detected numerous AT1-R–positive cells in the inner retina in vehicle-treated rats. After ischemia, the production of ROS was detected in retinal cells. However, pretreatment with captopril or candesartan suppressed the production of ROS. On the seventh postoperative day, the amplitudes of the ERG b-waves were significantly lower in the vehicle group than in the groups pretreated with captopril or candesartan.

Conclusions. The present findings demonstrate that ischemic damage promotes the expression of AT1-R in the inner retina. Both the ACE inhibitor and the AT1-R antagonist that were examined can block the stimulation of the AT1-R and attenuate the subsequent ischemic damage in the rat retina. (*Invest Ophthalmol Vis Sci.* 2010;51:3629–3638) DOI:10.1167/iovs.09-4107

The renin-angiotensin system is widely known as a major controller of systemic blood pressure. In this system, angiotensin II (Ang II) plays an essential role in regulating vasomotor tone and ion transport and thus can cause elevation of blood pressure. There are two Ang II receptor subtypes: Ang II type 1 receptor (AT1-R) and Ang II type 2 receptor (AT2-R).[1–4] Because major Ang II-related systemic functions are mediated by AT1-R signaling, its antagonist action is widely used for the treatment of hypertension and cardiac diseases. Chronic treatments that make use of angiotensin-converting enzyme (ACE) inhibitors or AT1-R antagonists have been reported to reduce stroke incidence and extend the lifespan in stroke-prone spontaneously hypertensive rats (SP-SHRs)[5,6] and to protect against cerebral ischemic damage in SHRs.[7,8] In the rat model of endotoxin-induced uveitis, Ang II has been shown to be a promoter of choroidal neovascularization (CNV) and retinal inflammation.[9–11] Ang II activates the NADPH-dependent oxidase complex, which is a major source of superoxide (O_2^-) and is upregulated in several pathologic conditions associated with oxidative stress.[12,13] Liu et al.[14] recently reported that administration of the AT1-R antagonist leads to a protective effect against cerebral ischemia. Moreover, recent evidence suggests that AT2-R may antagonize the action of AT1-R.[1] AT2-R is expressed in areas related to learning and control of motor activity and is found in fetal tissue. However, it is also present at low levels in adult tissue and is reexpressed in certain pathologic conditions, such as neuronal injury[15,16] and vascular injury,[17] suggesting that activation of AT2-R may play a pivotal role in the repair and regeneration of injured tissue. In addition, research is now suggesting possible therapeutic applications for AT2-R, particularly with respect to its protective effects against cerebral ischemia–induced neuronal death.[18–20]

The kallikrein system (KKS) has been implicated in various pathologic and physiological processes, including inflammation, allergies, blood coagulation, fibrinolysis, and the lowering of systemic blood pressure caused by vessel dilation and diuretic action.[21,22] Bradykinin, the central molecule of the KKS, is generated by kallikrein from kininogen, including vessel dilation and leakage.[23] There are at least two types of bradykinin receptors, B1 (B1-R) and B2 (B2-R).[24] B2-R has high affinity for the intact kinin whereas B1-R has greater affinity for the kinin metabolite but weak affinity for the intact kinin.[24,25] Most of the physiological functions of kinin are mediated by B2-R.[26]

Ischemia-induced injury to the retina, such as diabetic retinopathy and retinal vein occlusion, causes severe and long-lasting visual loss. These morbidities are hard to treat, and research is ongoing regarding possible therapeutic interventions.[27–31] In addition, many mechanisms of tissue injury-induced ischemia have been proposed.[32–35] Reactive oxygen species (ROS) trigger ischemic cell damage and lead to the hypersecretion of glutamate and aspartate.[34] An excess amount of glutamate produced under conditions of ischemia-reperfusion stimulates *N*-methyl-D-aspartate (NMDA), a subtype of the glutamate receptor,[35] and induces an influx of excess Ca^{2+} into the cell.[32,33] The purpose of the present study was to investigate the effects of the ACE inhibitor and an Ang II antagonist on neuronal death in retinal ischemia.

From the Departments of [1]Ophthalmology and [2]Neurobiology, Kagawa University Faculty of Medicine, Kagawa, Japan.

Supported by Grant-in-Aid 20592078 for Scientific Research from the Ministry of Education, Culture, Sports, Science, and Technology of Japan.

Submitted for publication June 8, 2009; revised October 7, 2009, and January 12, 2010; accepted January 30, 2010.

Disclosure: **K. Fukuda**, None; **K. Hirooka**, None; **M. Mizote**, None; **T. Nakamura**, None; **T. Itano**, None; **F. Shiraga**, None

Corresponding author: Kouki Fukuda, Department of Ophthalmology, Kagawa University Faculty of Medicine, 1750-1 Ikenobe, Miki, Kagawa 761-0793 Japan; snipeman@med.kagawa-u.ac.jp.

Materials and Methods

Animals

Female Sprague–Dawley rats, each weighing 200 to 250 g, were obtained from Charles River Japan (Yokohama, Japan). Female rats were used because preliminary results indicated no differences between male and female rats (data not shown). Rats were permitted free access to standard rat food (Oriental Yeast Co., Ltd., Tokyo, Japan) and tap water. Animal care and all experiments were conducted in accordance with the approved standard guidelines for animal experimentation of the Kagawa University Faculty of Medicine and adhered to the ARVO Statement for the Use of Animals in Ophthalmic and Vision Research.

Drugs

B2-R antagonist icatibant, AT2-R antagonist (PD123319), and bradykinin were obtained from Sigma-Aldrich (St. Louis, MO); the ACE inhibitor captopril was obtained from Wako (Osaka, Japan); and AT1-R antagonist candesartan was obtained from TRC (North York, Canada). All drugs except candesartan were dissolved in water; candesartan was dissolved in dimethyl sulfoxide (DMSO) to produce stock solutions that were then diluted to the final required concentrations. The final DMSO concentration never exceeded 5%. Drugs were administered intraperitoneally 30 minutes before the induction of ischemia with the exception of PD123319 (5 mg/kg/d), which was administered by subcutaneous osmotic minipump (Alzet model 1007D; Alza Corporation, Mountain View, CA) 1 day before ischemia. The minipumps were implanted subcutaneously into the midscapular region. As the control, animals were pretreated with intraperitoneal injections of vehicle (distilled water or 5% DMSO in PBS) 30 minutes before ischemia.

Ischemia

Rats were anesthetized with 50 mg/kg pentobarbital sodium (Abbott, Abbott Park, IL) injected intraperitoneally and 0.4% oxybuprocaine hydrochloride administered topically. The anterior chamber of the right eye was cannulated with a 27-gauge infusion needle connected to a reservoir containing normal saline. Intraocular pressure (IOP) was raised to 130 mm Hg for 45 minutes by elevating the saline reservoir. Only the right eye of each rat was subjected to ischemia. Retinal ischemia was indicated by whitening of the iris and fundus. The left eye of each rat served as the nonischemic control. Given that body temperature may influence ischemia-induced retinal ganglion cell death,[36] rectal and tympanic temperatures were maintained at approximately 37°C using a feedback-controlled heating pad (BRC, Nagoya, Japan) during the operation. After restoration of blood flow, temperature continued to be maintained at 37°C.

Histologic Examination

For the histologic examination, rats were anesthetized by intraperitoneal injection of pentobarbital sodium (50 mg/kg) 7 days after ischemia and were perfused intracardially with phosphate-buffered saline (PBS), followed by perfusion with 4% paraformaldehyde in PBS. Anterior segments, including the lens, were removed. Posterior eyecups were embedded in paraffin, and thin sections (5-μm thickness) were cut using a microtome. Sections were carefully cut to include the full length from superior to inferior along the vertical meridian through the optic nerve head. Each eye was mounted on a silane-coated glass slide and was stained with hematoxylin and eosin. Scleral thickness was measured to confirm that the sections were not oblique.

Morphometric analysis was performed to quantify ischemic injury. Five sections were selected randomly in each eye. One person with no previous knowledge of the treatments performed all the light microscopic (magnification, 10 × 100; Olympus BX-51, Tokyo, Japan) examinations. A microscopic image of each section within 0.5 to 1 mm superior of the optic disc was scanned. In each computer image, the thickness of the inner plexiform layer (IPL) and inner nuclear layer (INL) was measured. In each eye, the thickness of the IPL + INL was obtained as the mean of four measurements. For each animal, this parameter in the right eye was normalized to that in the intact left eye and was shown as a percentage.

Retrograde Labeling of Retinal Ganglion Cells

Seven days before kill, hydroxystilbamidine (Molecular Probes Inc., Eugene, OR) was injected bilaterally into the superior colliculi of anesthetized rats. The skull was exposed and kept dry and clean. After identifying and marking the bregma, a small window was drilled in the scalp in both the right and the left hemispheres. The windows were drilled to a depth of 3.6 mm from the surface of the skull and were located 6.8 mm behind the bregma on the anteroposterior axis and 1.5 mm lateral to the midline. Using a Hamilton syringe, 1.5 μL of 2% hydroxystilbamidine was slowly injected into the bilateral superior colliculi. After the skin was sutured over the wound, antibiotic ointment was applied.

Tissue Preparation and Assessment of RGC Survival

Animals were killed with an overdose of Nembutal at 1 week after 2% hydroxystilbamidine (Molecular Probes Inc.) application. Whole flat-mounted retinas were then assayed for retinal ganglion cell density. Rat eyes were enucleated and fixed in 4% paraformaldehyde for 10 hours at room temperature. After removal of the anterior segments, the resultant posterior eyecups were left in place. Subsequently, four radial cuts were made in the periphery of the eyecup, and the retina was then carefully separated from the retinal pigment epithelium. To prepare the flat mounts, the retina was dissociated from the underlying structures, flattened by making four radial cuts, and spread on a gelatin-coated glass slide. Labeled retinal ganglion cells (RGCs) were visualized under a fluorescence microscope (BX-51/DP70; Olympus) with an ultraviolet filter (blue-violet: 395–440 nm). Fluorescence-labeled RGCs were counted in 12 microscopic fields of retinal tissue from two regions in each quadrant at two different eccentricities, 1 mm (central) and 4 mm (peripheral) away from the optic disc. Software (Image-Pro Plus, version 4.0, Media Cybernetics, Bethesda, MD) was used to count the total number of RGCs in each eye. Changes in the densities of the RGCs were expressed as the RGC survival percentage, which was based on a comparison between the surgical and the contralateral control eyes. The specimens that were compared came from different retinal regions of the same animal.

Electroretinography

ERG responses were measured after overnight dark adaptation (at least 6 hours) using a recording device (Mayo Corporation, Aichi, Japan) 7 days after ischemia. Pupils were dilated with 0.5% tropicamide and 0.5% phenylephrine hydrochloride eye drops (Santen Pharmaceuticals, Osaka, Japan). All procedures were performed in dim red light, and the rats were kept warm during the procedure. A contact lens electrode was placed on the surface of the cornea. A differential electrode was placed under the skin on the forehead, and a neutral electrode was placed under the skin near the tail. Standard flash ERGs were obtained using a flash intensity of 3 cd · s/m^2 with a single flash. ERGs were obtained of both eyes for each animal. Ischemic damage to the retina was evaluated as the percentage of the a- and b-wave amplitudes from the right eyes subjected to ischemia compared with the nonischemic left eyes.

Immunohistochemistry for AT1-R

Eyes were enucleated at 6, 12, or 24 hours after 45 minutes of ischemia. Eyes were then fixed in 4% paraformaldehyde and embedded in paraffin. Retinal sections (5 μm) were rinsed in 100% ethanol twice for 5 minutes each, followed by a separate 95% ethanol and 90% ethanol rinse for 3 minutes each. The sections were then washed using PBS (pH 7.4) three times for 10 minutes each and were treated with 0.3% Triton X-100 in PBS (pH 7.4) for 1 hour After further washing

three times for 10 minutes each with PBS (pH 7.4), the sections were blocked in 3% normal horse serum and 1% BSA in PBS for 1 hour to reduce nonspecific labeling. Sections were incubated overnight at 4°C in a 1:100 dilution of rabbit polyclonal antibody against human AT1-R (Santa Cruz Biotechnology, Santa Cruz, CA) as the primary antibody in PBS containing 0.5% Triton X-100, 5% normal horse serum and 1% BSA. Control sections were prepared by omitting both the primary antibody and the rabbit IgG (1:1000; Vector Laboratories Inc., Burlingame, CA) and incubating only in PBS containing 0.5% Triton X-100, 5% normal horse serum, and 1% BSA overnight at 4°C. After they were washed in PBS for 50 minutes, sections were immersed in alkaline phosphatase (AP; Vectastain ABC-AP Kit; Vector Laboratories Inc.) for 30 minutes at room temperature, washed in PBS for 15 minutes, and processed using the avidin-biotin complex reagent (ABC Kit PK-6101; Vector Laboratories Inc.) for 1 hour at room temperature. Images were acquired using 40× objective lenses (DXM 1200; Nikon, Tokyo, Japan). Image editing software (PhotoShop, version 5.0; Adobe, Mountain View, CA) was used to adjust the brightness and contrast of the images.

ELISA for AT1-R

Eyes were immediately enucleated 6, 12, and 24 hours after 45 minutes of ischemia, and the retina was carefully isolated. Retinas were put into buffer (IBLysis-I; IBL, Takasaki, Japan) and homogenized. These samples were centrifuged at 10,000 rpm for 10 minutes; the supernatant fluid was then removed and put into each well of a 96-well plate. After 10 μg/mL rabbit anti-AT1-R antibody (Santa Cruz Biotechnology, Santa Cruz, CA) was added to each well, the plates were covered and kept at 4°C overnight. On the next day, each well was washed with PBST (PBS + 0.05% Tween 20), followed by addition of horseradish peroxidase-conjugated anti-rabbit antibody into each well and further incubation at 4°C for 1 hour. Subsequently, the samples were washed with PBST after which 100 μL substrate (TMBS; IBL) was added, followed by a 30-minute period for development at room temperature in the dark. After the reaction was stopped with 100 μL 1 N H_2SO_4, the OD450 was immediately measured.

Fluorescence Labeling of ROS

To investigate the production of ROS, we injected 5 mg/kg dihydroethidium (DHE; Sigma-Aldrich) in 5% DMSO in PBS intraperitoneally 15 minutes before ischemia. A 0.3-mL aliquot of distilled water, 1 mg/kg candesartan, or 10 mg/kg captopril was administered intraperitoneally 30 minutes before ischemia. Eyes were enucleated 15 minutes after ischemia and then embedded in the OCT compound (Sakura Finetek, Torrance, CA), after which cryosections (20 μm) were prepared. Sections were examined with a microscope (Radiance 2100/Rainbow; Carl Zeiss, München, Germany) using a laser set (excitation laser 514 nm; emission laser >580 nm).

Detection of O_2^- by Formazan Deposition

Detection of O_2^- by formazan deposition was performed by reduction assay (Nitro Blue Tetrazolium Chloride [NBT]; Wako Chemicals, Tokyo, Japan) with slight modification of the methods of Imai et al.[37] Known amounts of KO_2 (Sigma-Aldrich) were dissolved and diluted with 12 mM dicyclo-hexano-16-crown-6 (crown-6; Sigma-Aldrich) DMSO solution. NBT was also dissolved in 12 mM crown-6 DMSO solution to a final concentration of 0.4 mM (NBT solution). Known amounts of KO_2 solution were added to 1 mL NBT solution, resulting in the immediate formation of O_2^--reduced NBT and insoluble formazan. The solution was analyzed by spectrophotometer (UM3300; Hitachi, Tokyo, Japan) at a wavelength of 572 nm. After obtaining the calibration curve, O_2^- in the retina was determined by extraction of the NBT solution. Rats were killed immediately after the experiment, and the retinas were removed as soon as possible. Each retina was immersed in 1 mL NBT solution for 5 minutes, and then the supernatant was analyzed by the spectrophotometer at 572 nm.

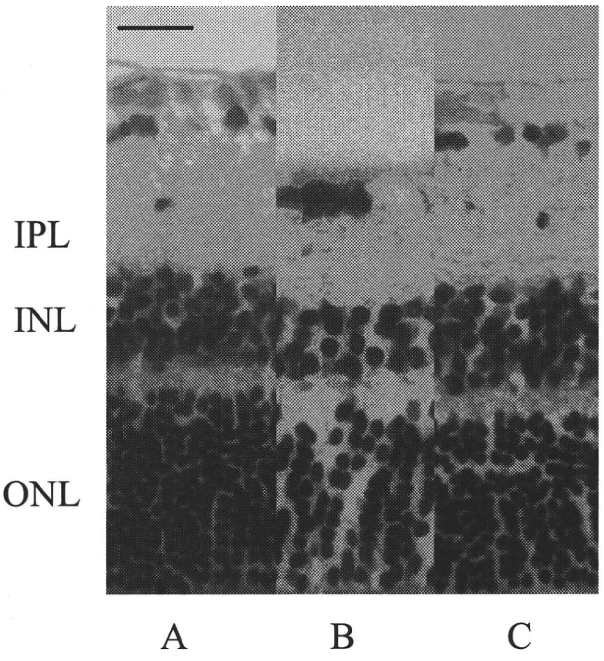

FIGURE 1. Light micrographs of a cross-section through normal rat retina (**A**) and 7 days after ischemia without captopril pretreatment (**B**) or with 10 mg/kg of captopril pretreatment (**C**). Each microscopic image of the retina was scanned within 0.5 to 1 mm superior of the optic disc. Scale bar, 10 μm.

Statistical Analysis

Image analysis was performed (Image-Pro Plus software, version 4.0; Media Cybernetics) to assess the altered ROS reaction area. We used the total red-stained area as the indicator of ROS production.

All data are presented as the mean ± SD. Data were analyzed using an independent Student's *t*-test or a Dunnett's multiple comparison test, as appropriate. $P < 0.05$ was considered statistically significant.

RESULTS

Histologic Changes in the Retina after Ischemia with Captopril

Figure 1A shows a normal retina with no ischemic procedures. Light microscopic photographs were taken 7 days after ischemia in retinas pretreated with distilled water (Fig. 1B). Significant reduction in the thickness of the IPL + INL to 68.9% ± 18.5% ($n = 6$) after ischemia was observed. Figure 1C shows the retina 7 days after ischemia in retinas pretreated with captopril (10 mg/kg). In animals pretreated with 0.1, 1, or 10 mg/kg captopril, the thickness of the IPL + INL was 68.6% ± 14.5% ($n = 6$), 71.6% ± 7.2% ($n = 5$), and 96.7% ± 23.2% ($n = 6$) of the control, respectively (Fig. 2). Administration of 10 mg/kg captopril significantly prevented reduction in the thickness of the IPL + INL ($P < 0.05$). Administration of 10 mg/kg captopril 30 minutes after ischemia also provided a neuroprotective effect (95.2% ± 21.1%, $P < 0.05$, $n = 4$; Fig. 2).

Effect of Candesartan or PD123319 on the Retina after Ischemia

Figure 3A shows a normal retina with no ischemic procedures. Light microscopic photographs were taken 7 days after ischemia in retinas pretreated with 5% DMSO in PBS (Fig. 3B). Significant reduction in the thickness of the IPL + INL was

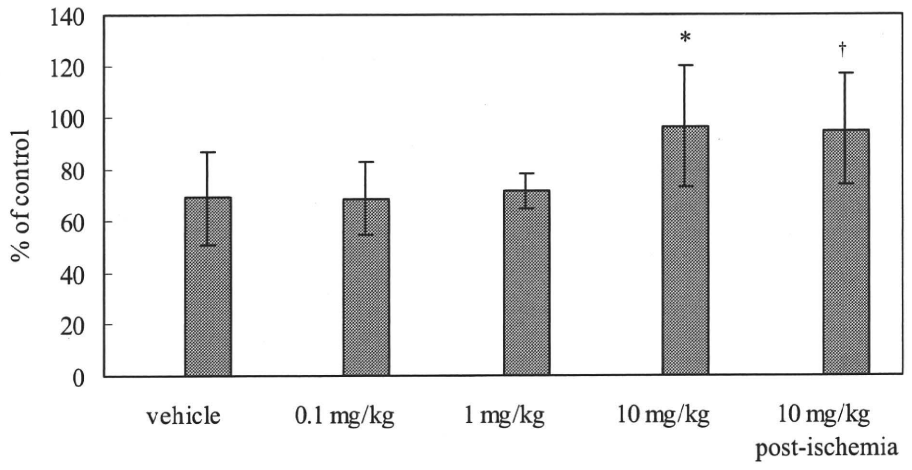

FIGURE 2. Percentage change relative to control values in the thickness of the IPL + INL 7 days after ischemia without captopril pretreatment or with 0.1, 1, and 10 mg/kg captopril pretreatment or 10 mg/kg captopril postischemic treatment. Data express the mean ± SD. $^*P < 0.05$ versus vehicle (Dunnett's multiple comparison test). $\dagger P < 0.05$ versus vehicle (independent Student's *t*-test).

observed. Figure 3C shows the retina 7 days after ischemia in retinas pretreated with candesartan (1 mg/kg). In animals pretreated with 0.1 or 1 mg/kg candesartan, the thickness of the IPL + INL was 81.2% ± 24.7% ($n = 5$) or 91.3% ± 23.7% ($n = 7$) of control, respectively (Fig. 4A). Administration of 1 mg/kg candesartan reduced ischemic damage to the retina ($P < 0.05$). Administration of 1 mg/kg candesartan 30 minutes after ischemia also provided a neuroprotective effect (89.3% ± 14.6%, $P < 0.05$, $n = 4$; Fig. 4A).

A 5-mg/kg/day dose of PD123319 administered subcutaneously by osmotic minipump showed no protective effect against retinal ischemic damage (Fig. 4B). The thickness of the IPL + INL was 78.4% ± 19.4% ($P = 0.1$; $n = 5$).

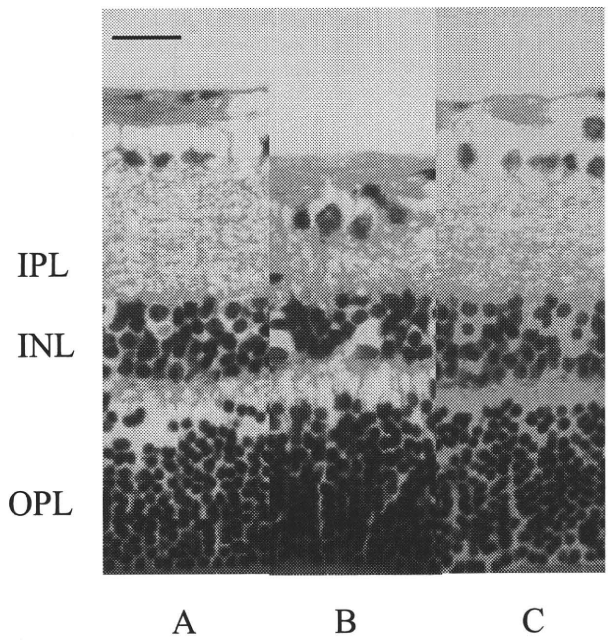

FIGURE 3. Light micrographs of a cross-section through normal rat retina (**A**) and 7 days after ischemia without candesartan pretreatment (**B**) or with 1 mg/kg candesartan pretreatment (**C**). Each microscopic image of the retina was scanned within 0.5 to 1 mm superior of the optic disc. Scale bar, 10 μm.

Effect of Bradykinin or Bradykinin B2 Receptor Antagonist on the Retina after Ischemia

Pretreatment with 1 mg/kg bradykinin ($n = 5$) or 0.01 to 1 mg/kg icatibant (each dose; $n = 5$) showed no protective effect against retinal ischemic damage (Fig. 5). However, coinjection of captopril (10 mg/kg) with icatibant (0.1 mg/kg) did have a protective effect against retinal ischemic damage ($P < 0.05$; $n = 3$; Fig. 5). Even so, this coinjection of captopril (10 mg/kg) with icatibant (0.1 mg/kg) was not significantly different from the injection of icatibant (0.1 mg/kg) by itself ($P = 0.057$; independent Student's *t*-test).

Effect of Captopril or Candesartan on RGC Survival

Figure 6A shows representative results of the RGC labeling in the vehicle-, captopril-, and candesartan-treated rats. Compared with the vehicle-treated rats, RGC death seemed to be mild in the captopril- and candesartan-treated rats. RGC survival rates in the central retinas of the eyes with ischemia were 53.2% ± 11.3% in the vehicle-treated group ($n = 6$), 72.9% ± 13.2% in the captopril-treated group ($P = 0.02$; $n = 6$), and 71.9% ± 9.9% in the candesartan-treated group ($P = 0.03$; $n = 6$; Fig. 6B). In the peripheral retina, RGC survival rates in the eyes with ischemia were 54.2% ± 7.5% in the vehicle-treated group, 73.5% ± 10.9% in the captopril-treated group ($P = 0.02$), and 75.2% ± 15.4% in the candesartan-treated group ($P = 0.01$; Fig. 6B).

Effect of Captopril or Candesartan on Retinal Function

Recoveries of a- and b-wave amplitudes are shown in Figure 7. On the seventh postoperative day, a-wave amplitude percentages were 41.6% ± 6.0% in the vehicle-treated group ($n = 6$), 47.2% ± 8.0% in the captopril-treated group ($n = 6$), and 43.4% ± 6.5% in the candesartan-treated group ($n = 6$; Fig. 7A). Percentages for b-wave amplitude were 28.3% ± 4.3%, 38.2% ± 8.0%, and 39.0% ± 6.4%, respectively (Fig. 7B). Recovery rates of b-wave amplitude in the eyes treated with captopril or candesartan were significantly higher than in the vehicle group. There was no significant difference in the recovery rates of the a-wave amplitude either between the captopril group and the vehicle group or between the candesartan group and the vehicle group. Both a- and b-wave amplitudes in the nonischemic eyes were stable and were essentially equal before and after ischemia.

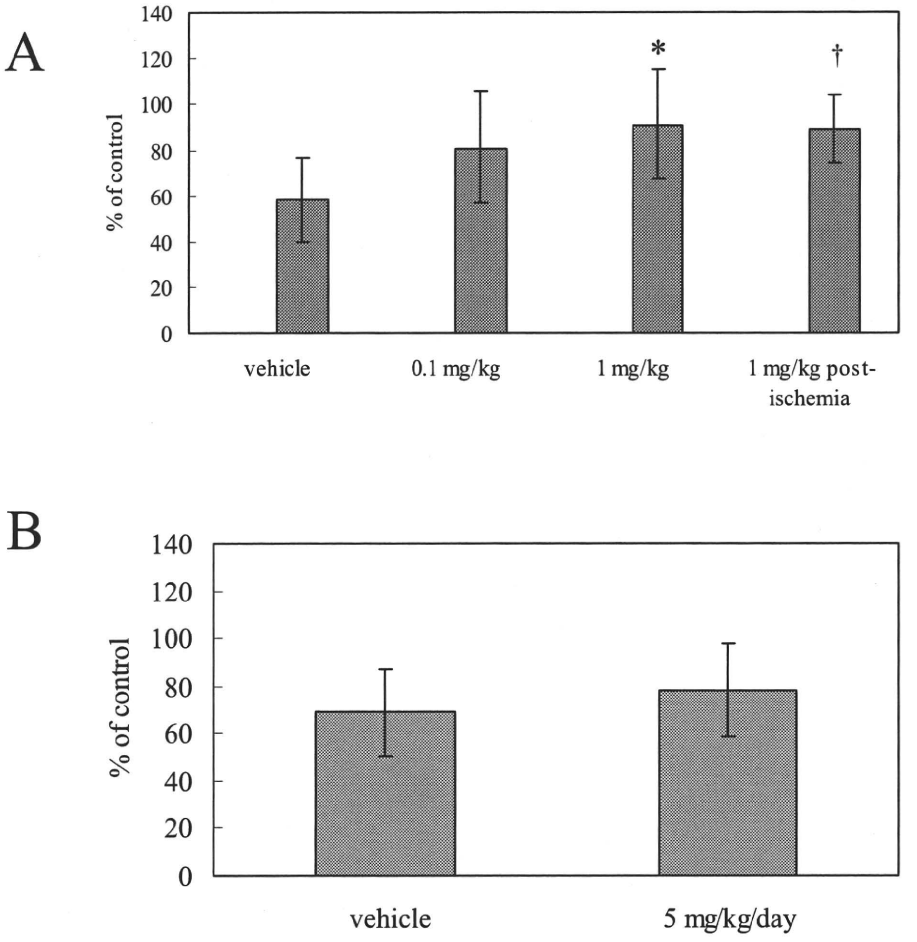

FIGURE 4. Percentage change relative to the control values in the thickness of the IPL + INL 7 days after ischemia without candesartan pretreatment or with 0.1 and 1 mg/kg candesartan pretreatment or 1 mg/kg candesartan postischemic treatment (**A**) or 5 mg/kg/day PD123319 pretreatment (**B**). Data express the mean ± SD. *$P < 0.05$ versus vehicle (Dunnett's multiple comparison test). †$P < 0.05$ versus vehicle (independent Student's *t*-test).

AT1-R Tissue Localization in the Retina after Ischemia

We examined the expression of AT1-R in the retina at 6, 12, and 24 hours after 45 minutes of ischemia (Fig. 8). Figure 8A shows the localization of AT1-R in the normal retina. Although retinal vessels were positive for AT1-R, AT1-R expression was not detected in any layer in the normal retina. However, in the postischemic retina (Figs. 8B–D), immunostaining for AT1-R was detected primarily in the IPL and INL. AT1-R expression increased gradually from the baseline and peaked between 6 and 12 hours after ischemia (Figs. 8C, 8D).

AT1-R Expression in the Retina after Ischemia

Protein levels of AT1-R in the retina were upregulated by ischemia/reperfusion injury (Fig. 9). In the normal retina, the AT1-R protein level was 0.034 ± 0.005 ng/mL ($n = 6$). How-

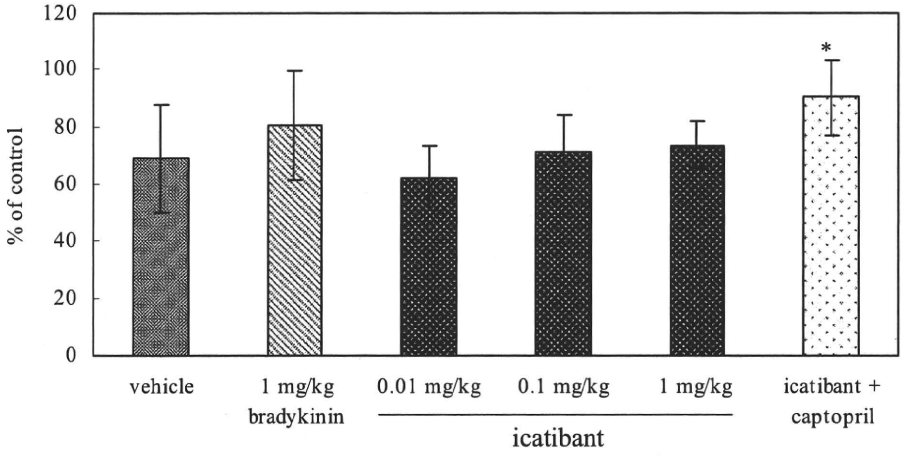

FIGURE 5. Percentage change relative to control values in the thickness of the IPL + INL 7 days after ischemia with pretreatment with vehicle; 1 mg/kg bradykinin; 0.01, 0.1, or 1 mg/kg icatibant; or 0.1 mg/kg icatibant coinjected with 10 mg/kg captopril. Data express the mean ± SD. *$P < 0.05$ versus vehicle (independent Student's *t*-test).

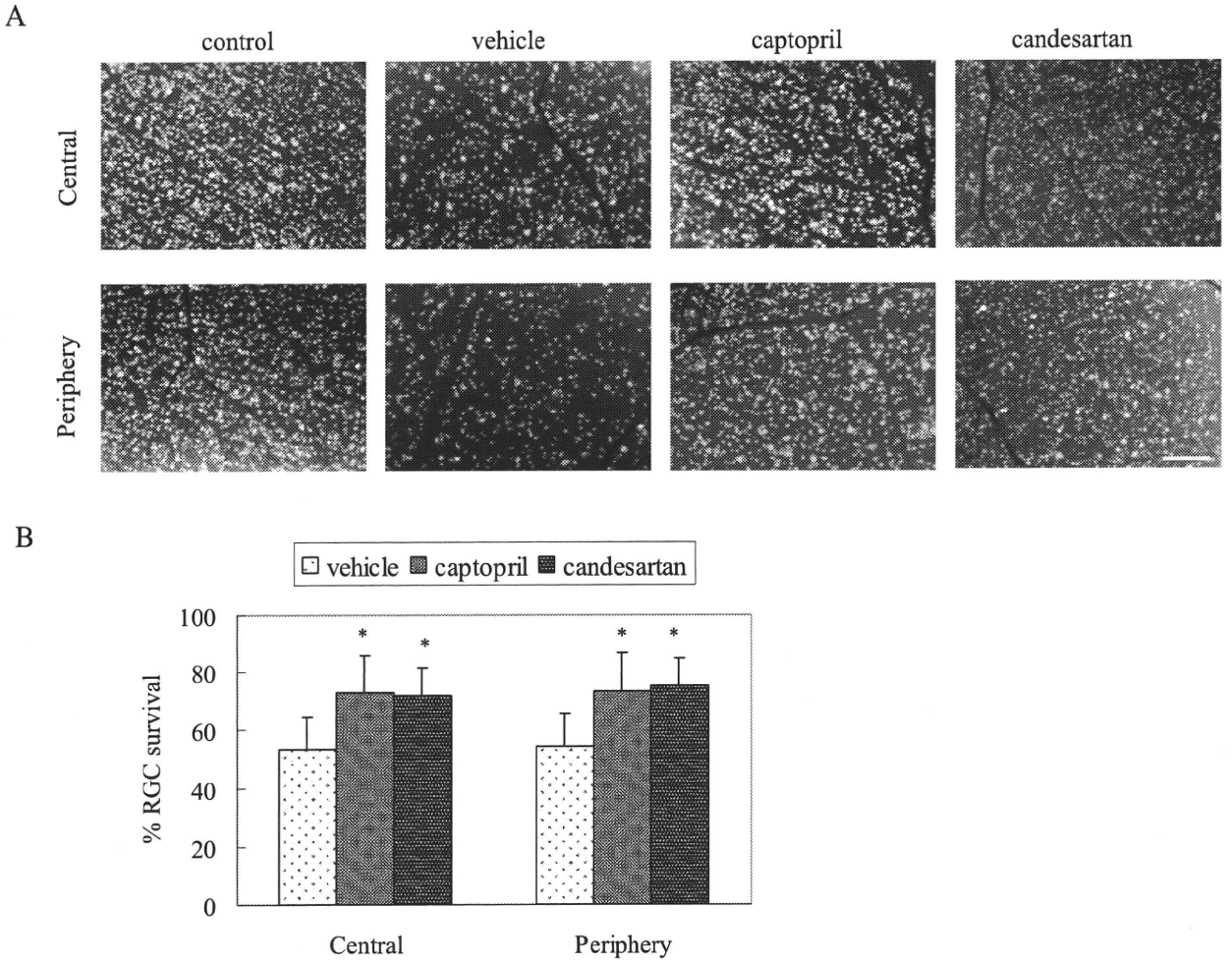

FIGURE 6. Effect of captopril or candesartan on ischemia-induced retinal ganglion cell death. (**A**) Retrograde labeling of RGCs in nonischemic eyes and 7 days after ischemic injury after administration of vehicle, captopril, or candesartan. Micrographs of the central and peripheral areas were taken approximately 1 and 4 mm from the optic nerve head. Scale bar, 20 μm. (**B**) RGCs were counted in the central and peripheral areas at approximately 1 and 4 mm from the optic nerve head. Graph depicts the mean ± SD of six animals treated with vehicle, six animals treated with captopril, and six animals treated with candesartan. Data express the mean ± SD of six independent experiments. $^*P < 0.05$ versus vehicle (Dunnett's multiple comparison test).

ever, AT1-R expression peaked between 6 (n = 4) and 12 (n = 4) hours after ischemia and then dramatically decreased by 24 hours after ischemia (n = 4).

ROS Activation by Ischemia

We tested whether ROS were suppressed by treatment with 10 mg/kg captopril or 1 mg/kg candesartan. For this purpose, we used DHE staining because DHE specifically reacts with intracellular O_2^-, a ROS, and is converted to the red fluorescent compound ethidium in nuclei. In the postischemic retina, DHE fluorescence was clearly upregulated in retinal neuronal cells, and this up-regulation was efficiently suppressed by captopril or candesartan (Fig. 10A). Figure 10B shows the quantification of the color areas expressed as a percentage change (n = 4 each). Mean ROS activation was significantly suppressed by treatment with captopril or candesartan.

Detection of O_2^- in the Retina after Ischemia

Figure 11 shows the amount of O_2^- produced after ischemia with pretreatment of vehicle, 10 mg/kg captopril, or 1 mg/kg candesartan. The amount of O_2^- produced in the retina was 6.73 ± 0.83 μg (control; n = 4), 12.10 ± 1.89 μg (vehicle; n = 4), 7.01 ± 0.44 μg (captopril; n = 4), and 7.68 ± 0.80 μg (candesartan; n = 4). The mean detection of O_2^- was significantly suppressed by treatment with captopril or candesartan.

Discussion

We have demonstrated that ischemic injury to the rat retina can be prevented by pretreatment with an ACE inhibitor or an AT1-R antagonist. This result indicates that the local rennin-angiotensin system (RAS) is one of the main pathways of retinal ischemic injury. Furthermore, our results revealed tissue localization of AT1-R upregulation after ischemia in the retina, which further suggests an involvement of the local RAS in ischemic injury and subsequent cell death.

Glutamate is released from the retina during and after ischemia by raising the IOP.[29,35,38] Glutamate has been widely known to induce selective damage in the inner layers of the retina.[34,39] The major causes of cell death after activation of the